WORCESTER POLYTECHNIC INSTITUTE

A Cell Spheroid Model of Calcific Aortic Valve Disease: The Role of Apoptosis and Oxidative Stress

by

Colin Coutts

A thesis submitted in partial fulfillment for the

degree of Master of Science

in

Biomedical Engineering

July 2021

APPROVED:

_____

Professor Marsha W. Rolle, Thesis Committee Chair

_____

Professor Kristen L. Billiar, Thesis Advisor

_____

Professor Jeannine M. Coburn, Thesis Committee Member

Acknowledgements

I would like to acknowledge everyone who played a role in my academic accomplishments. First, my parents, who supported me with love and understanding. Without you, I could never have reached this current level of success. Secondly, my committee members, each of whom has provided advice and guidance throughout the research process. Specifically, I would like to thank Professor Kristen Billiar for advising this project and providing the space and materials to work with. I would also like to thank my mentor Mahvash Jebeli for guiding me through the project as well as Jyotsna Patel for providing and helping with much of the histology. Without all your help and guidance this project would not have been possible.

Abstract:

Calcific aortic valve disease (CAVD) is the most common heart valve diseases among aging populations. There are two reported pathways of CAVD: osteogenic and dystrophic, the latter being more prevalent. Current two-dimensional (2D) in vitro CAVD models have shed light on the disease but lack three-dimensional (3D) cell and ECM interactions, and current 3D models induce calcification using osteogenic media. The goal of this work is to develop a 3D dystrophic calcification model. We hypothesize that, as with 2D models, mechanical stress-induced apoptosis is integral to calcification and that oxidative stress plays a minor role. We model the cell aggregation observed in CAVD by creating porcine valvular interstitial cell spheroids in agarose microwells. Upon culture in standard growth media, calcium nodules form within the spheroids. In contrast, supplementation with ascorbic acid (AA) virtually eliminates calcium buildup. As this effect has previously been attributed to the antioxidant properties of AA rather than its stimulation of extracellular matrix (ECM) production, other antioxidants (Trolox and Methionine) were also used as supplements as these reduce oxidative stress while having differing effects on ECM formation. All three antioxidants significantly reduced calcification as measured by Von Kossa staining, with percent calcification per area of AA, Trolox, Methionine, and the non-antioxidant-treated control on day 7 equaling 0.17%, 2.5%, 6.0%, and 7.7%, respectively. As AA inhibited calcification significantly more than the other antioxidants, other effects of AA such as ECM stimulation may also play a role. Inhibiting apoptosis with Z-VAD also significantly reduced calcification demonstrating that the calcification observed in this model is dystrophic rather than osteogenic. We conclude that while not the sole factor, oxidative stress plays a crucial role in calcification in this 3D in vitro model and may be a viable therapeutic target for CAVD.

Table of Contents

Table of Figures

Introduction:

  Calcific aortic valve disease (CAVD) is a common heart valve disease affecting approximately 2–4% of people over the age of 65 and is characterized by the thickening of fibrotic leaflets as well as the formation of calcific nodules [1]. While there are several types of treatments, the current standard of care for CAVD is to replace the valve through surgery. This treatment, however, has short term risks such as the dangers of surgery, and long-term risks such as morbidity and increased complications attributed to anticoagulation as well as the need for reoperation because of the limited lifespan of prosthetic valves [2]. Transcatheter aortic valve replacement (TAVR) is another option currently offered for patients with excess operative risk, and it is becoming a more popular option due to procedure being significantly less invasive compared with surgical aortic valve replacement; however, TAVR suffers from complications as well [3]. The overall problem remains, as there are no medical therapies for CAVD as alternatives to surgery [2]. Originally, CAVD was presumed to be a degenerative disease that affected older populations since their valves have been opening and closing every second of a person's life [1]. This process, however, is now known to be a more activated cell-driven process [1].

  There are two types of cell-driven processes that lead to the calcification of the valve. The first is osteogenic calcification which occurs when valvular interstitial cells (VICs) adopt an osteoblast-like phenotype which will produce an osteoid matrix [4]. While this is the better understood cause of calcification, it is only responsible for 13% of all cases [4]. The other process is dystrophic calcification, which is responsible for 83% of all cases, and is caused when VICs in their natural quiescent state become activated and take on a myofibroblast-like phenotype, which then calcify through an apoptosis-dependent mechanism [4]. Due to the process now being understood as an active process, via pro-osteogenic and apoptotic pathways, researchers believe there may be a way of inhibiting the calcification [1].

  While the mechanism for VIC's undergoing apoptosis is not currently known, it has been shown by multiple research groups that apoptosis plays a role in calcification in 2D in vitro experimental systems. One example comes from Fisher et al. who reproducibly formed 2D aggregates, apoptosis occurred in the center, and subsequently calcific nodules formed [5]. Through using Z-VAD to block apoptosis, the group observed a significant reduction in the number of calcific nodules revealing the importance of apoptosis to the calcification process [5]. Another in vitro model showed the same using VICs, where they were seeded at high density into culture dishes and then supplemented with TGF-β1 [6]. VICs activated to the myofibroblast phenotype and formed cell aggregates. Apoptosis then occurred within the middle of the aggregates which began calcifying [6]. This method however had limitations associated with the consistency and reproducibility of those 2D aggregates. Similar results were shown by Yip et al. who found apoptosis led to calcification on stiff substrates, and that it can be attributable to local contraction of the cell layer resulting from increased cytoskeletal tension, which is then released on aggregation [7]. This was tested through constrained collagen gels seeded with VICs where they observed a significant increase in the number of apoptotic cells [7]. These studies all had the

limitation that they were studied in 2D which 3D cell-cell and cell-matrix interactions found in-vivo.

Using micro-contact printing, our group was able to consistently reproduce cell aggregation with myofibroblastic markers, apoptosis, and calcium accumulation [8]. The method was found to be highly reproducible as 70% of aggregates stained positive for Alizarin Red S after one week in culture, and mineralized calcium-positive nanoparticles were found within the VIC aggregates, which had an increase in area on the aggregate staining for the apoptotic pathway maker caspase [8]. This study was useful in understanding not only calcification, but also the VIC aggregate formation and characteristics of those aggregates. This method is also limited for the same reason as 2D studies are not able to mimic the 3D environment of a heart valve.

Several groups have begun researching CAVD using 3D in vitro models, typically with the use of a hydrogel made from polymers such as photocrosslinked hyaluronic acid (HA) or gelatin. Duan et al. used a 3D HA hydrogel which through adjusting the UV light exposer and photocrosslinking time has an adjustable matrix stiffness, which the researchers were able to use in order to investigate the dynamic interplay between human aortic valvular interstitial cells phenotype and matrix biomechanical remodeling in response to physiological, activation and calcification prone environments [9]. Their results suggest that constructs with initially valve leaflet layer-like stiffness significantly promote myofibroblastic phenotype [9]. This would suggest that increasing stiffness leads to an increase in cells beginning the path towards dystrophic calcification. Duan et al. was researching a 3D hydrogel with VICs, however the cells were not aggregated which has been shown as integral to calcification. Hjortnaes et al., developed another promising 3D using a hydrogel made from photocrosslinked hyaluronic acid and gelatin, where they found that VICs encapsulated into the 3D hydrogels showed the myofibroblast-like response only occurs when exposed to exogenous environmental cues, and there was no apoptotic driven calcification [10]. In another 3D model, Monroe et al. used a laminar, filter paper-based cell culture system which was established previously as a method for analyzing VIC migration as well as protein expression [11]. A key takeaway was that researchers were able to determine that the relative amount of fibrillar collagen within a 3D construct would dictate the osteogenic capacity of VICs that reside in the construct [11]. Butcher et al. formed a 3D model using collagen I solution which formed a fibrillar gel network, who found that a differences in protein and GAG content indicated an ability of the valvular interstitial cell to synthesize matrix in 3D culture, without the need of biochemical or mechanical stimulation [12]. Mabry et al. developed a 3D model where porcine aortic VICs were encapsulated within MMP-degradable, PEG-based hydrogels using a photoinitiated thiol-ene reaction [13]. From this model they were able to determine that the substrate modulus had an influence on VIC morphology and calcification, where stiffer substrates lead higher levels of calcium deposition [13]. Other groups have utilized dissected porcine aorta that are then cultured in standard or osteogenic media, where they were only able to induce calcification with the osteogenic supplementation [14]. Key limitations revolving around these models are that they all use osteogenic media and thus do not provide insight into the more prevalent dystrophic pathway. Also, many models encapsulate VICs as single cells, which does not mimic the 3D in-vivo cell-cell interactions.

As 2D models are unable to mimic a the complex valve environment and 3D models employ single cells to study osteogenic calcification, there is a need for a 3D model in which dystrophic calcification can be studied. Interestingly, Roosens et al., in their attempt to engineer healthy valve tissues by generating valvular interstitial cell aggregates, found that the 3D aggregates calcified when grown in standard media. They were able to overcome this "limitation" by supplementing the media with ascorbic acid which they postulated acts as an antioxidant protecting the cells against oxidative stress-induced cell damage [15]. Antioxidants have been shown to have protective affects against apoptosis, which as previously stated has been shown to be integral to calcification in 2D [16]. This VIC spheroid model is a potentially powerful system in which to study the mechanisms of dystrophic calcification in 3D culture.

The goal of this study is to better understand the role of apoptosis and antioxidants in the formation of calcific nodules using a 3D cell spheroid model of dystrophic calcification. Based on literature about apoptosis being integral to calcification in 2D we hypothesize that it could be recapitulated in 3D through blocking apoptosis in aggregates. We also hypothesize that antioxidants will have a protective affect against oxidative stress which will block or prevent calcium buildup. Aggregates formed in non-adherent wells will be subjected to different conditions and stained with Von Kossa to visualize and quantify the calcium buildup. Specifically, we tested different antioxidants with known protective effects against oxidative stress to determine if there was a direct impact on aggregate calcium buildup. Aggregates as well as VICs were also subject to other histological stains in order to visualize collagen, live and dead cells, and apoptosis.

Materials and Methods:

Cell Cultures

Normal porcine aortic valvular interstitial cells (PAVICs) were extracted form porcine hearts obtained from a local abattoir (Blood Farm, Groton, MA) within three hours of tissue harvest per published protocols and used in experiments from passages 4-9 [17]. Cell cultures were maintained in DMEM medium (Gibco) containing 1% antibiotics and 5% fetal bovine serum (Gibco). All cell cultures were maintained at 37°C and 10% CO_2 atmosphere.

Aggregate Formation

Aggregates were formed using Microtissues® negative molds with 300μm x 800μm wells based on Roosens et al. [15]. Negatives were filled with 3% w/v Agarose solution made with SeaKem® LE Agarose in DPBS 1x (Corning), then once solidified one million PAVICs were evenly distributed in 200μL to fill the 256 wells per mold (Figure 1). Each mold was

cultured in a separate dish or well and standard DMEM or DMEM supplemented with antioxidants was replenished every 2-3 days.
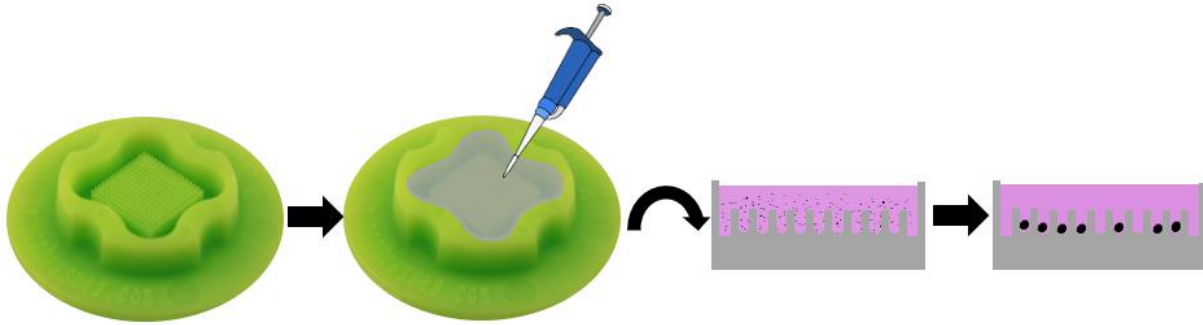

Figure 1 Aggregate Formation: Method of forming aggregates through filling a negative mold with non-adherent agarose, then filling the mold with one million cells evenly suspended in DMEM. Cells will then settle into the bottom of the 256 wells and form aggregates in roughly 70% of the wells.

Calcium Staining

Von Kossa Staining was performed to visualize calcium buildup within aggregates per Deegan et al. [18]. Aggregates were fixed in 10% Formalin (Sigma Aldrich) then put under UV light for 20 minutes in 1% aqueous silver nitrate (MP Biomedicals). Excess silver nitrate was removed using 5% sodium thiosulfate (Thermo Fisher Scientific) for 5 minutes. Aggregates were counterstained using 0.1% nuclear fast red (Polysciences Inc.) for 3 minutes. Aggregates were then washed and imaged in 70% ethanol. Calcium buildup was quantified by optimizing the threshold of each aggregate individually (ImageJ) leaving the calcific nodules as black areas and the surroundings as white (Figure 2). These calcific nodule areas were measured to determine the overall area of the calcified regions using particle analyzer. This was then divided by the total area of the aggregate, measured by tracing the edges of the aggregate, to give the percent calcification per area (PCPA) of the aggregate.
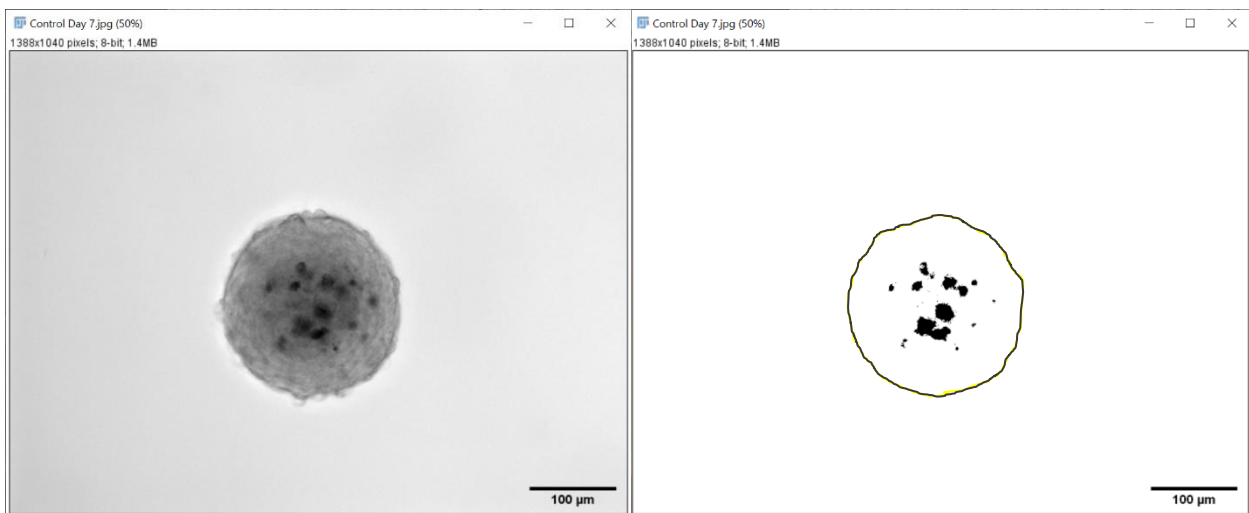

Figure 2 Calcium Quantification: Quantification of calcium buildup using ImageJ with phase image (left) and thresholded/binarized image to quantify calcific nodules (right).

Cell Viability

Cell Viability was measured using alamarBlue[TM] (Thermo Fisher Scientific). AlamarBlue[TM] is an important redox indicator that is used to evaluate metabolic function and cellular health [19]. This works through resazurin which is used as an oxidation-reduction indicator that undergoes colorimetric change in response to cellular metabolic reduction [19]. Therefore, the initial blue color that AlamarBlue[TM] adds to the media will be reduced in color if the cells are healthy and undergoing more normal cell cycles. Cells were washed with PBS 1X (Corning) and media was replenished with 10% alamarBlue[TM] and allowed to culture for 8 hours. Testing was done by putting a 96-well plate into a plate reader which measured fluorescence signals at an excitation wavelength of 530–560 nm and an emission wavelength at 590 nm [19]. Another means to measure cell viability was through Live/Dead staining with Propidium Iodide (Thermo Fisher Scientific) for dead and calcein (Thermo Fisher Scientific) for live.

Blocking Apoptosis

Apoptosis in aggregates was blocked by supplementing DMEM with 20uM Z-VAD for 5 days before seeding in agarose molds per Cirka et al. [8]. Z-VAD was added at the same concentration for replenishing the media for the duration of the experiment. To ensure Z-VAD was properly blocking apoptosis the cells were stained for caspase (Invitrogen).

Measuring Caspase

Staining aggregates for caspase (CellEvent Caspase 3/7 - Invitrogen) then imaging using a fluorescent microscope at ~502/530nm revealed apoptosis. Staining for caspase 3 and caspase 7 covers the major executioner caspases [20]. Using ImageJ, the aggregates were outlined and the integrated density of the gray value was measured, then a small circle next to the aggregate was created to measure the background grey value (Figure 3). The corrected total cell fluorescence was then calculated with the equation: (integrated density)-(area of aggregate) *(mean background). Finally dividing that number by the area gave us the corrected total cell fluorescence per area.
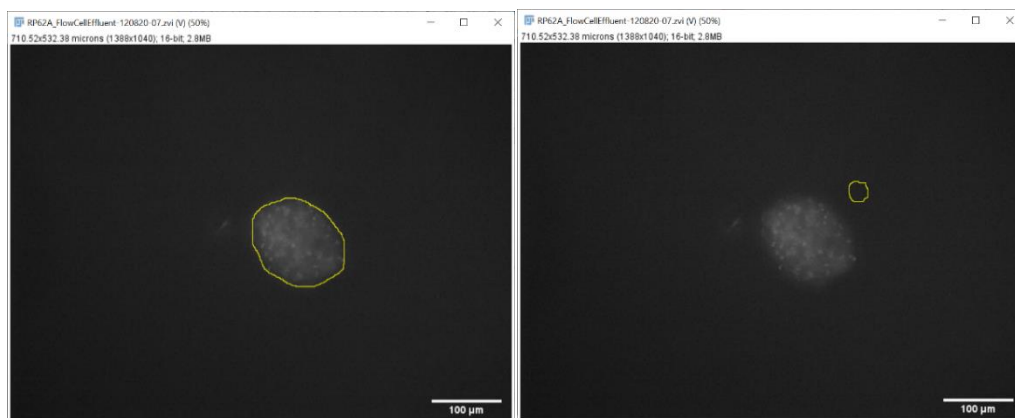

Figure 3 Caspase Quantification: To measure corrected total cell fluorescence aggregates were outlined, measured, and then also measured outside of the aggregate to determine background.

Inducing Oxidative Stress

To induce oxidative stress on the cells, culture media was supplemented with hydrogen peroxide. Concentrations of hydrogen peroxide tested on the cells were based on literature on inducing stress on fibroblasts; these studies indicate that a range between 0-1mM is effective [21]. Effective concentrations were defined as occuring when cells were seen to have reduced proliferation as well as visible dead cells (through Live/Dead staining), without killing majority of the population [21]. To determine ideal concentrations for our cells, VIC monolayers were incubated with concentrations of H_2O_2 in DMEM from 1μM-750μM once they reached roughly 80% confluency. The cells were incubated for 24 hours followed by a Live/Dead (Invitrogen) stain to determine overall viability of cells.

Antioxidant Selection and Supplementation

To determine the effects of antioxidants on calcification, Trolox and Methionine were incorporated in the study for their known protection against ROS. It was important for this selection to ensure that these two antioxidants were able to protect the cells without having similar effects on inducing ECM production as AA. Trolox and AA are in the same family as they are vitamin E and vitamin C, respectively. Trolox, however, does not increase formation of collagen in fibrous tissue as AA, and has been shown to be more potent in promoting regenerative capacity in comparison to ascorbic acid [16]. Both are capable of significantly reducing intracellular oxidative stress. Methionine, on the other hand, is an essential amino acid in humans and is largely involved in the production of cysteine, which is used to build proteins in the body [17]. This reagent has been shown to have great effects on improving cellular oxidative balance as well as mediating oxidative stress, where it targets ROS directly by being oxidized to methionine sulfoxide [17]. Initial testing concentration were chosen based on literature showing effectiveness of the antioxidants at 100-200μM for Methionine and 1mM for Trolox [22, 23]. Trolox was not soluble in DMEM and was therefore dissolved in 70% ethanol and added to DMEM with the ethanol being no more 0.5% of the final volume.

Microscopy

All images shown were taken using a Zeiss Microscope. Phase and fluorescent images were taken using 10x and 20x magnification and is specified with the images. During imaging of Von Kossa stained aggregates there was a shift in method to transmitted light without the phase ring to better visualize the calcium deposits; images with darker background had a phase ring and lighter backgrounds did not have phase contrast. Both techniques were able to visualize calcium deposits, however the later used method produced better images of the deposits within the aggregates. These two techniques were still able to be compared as the overall calcium deposits were visible in both.

Statistical analysis

One-way ANOVA on ranks were performed due the non-normality of the data sets and post-hoc pairwise comparisons were completed using the Dunn's test. This means of analysis was done to determine the significance comparing each group to all others of the same study

individually. Descriptive statistics are reported as the mean plus or minus the standard deviation and $p < 0.05$ was considered statistically significant. All statistics were performed on replicates of at least 10 aggregates (n≥10) unless otherwise specified. For each study, however, all 10 aggregates came from the same sample micro mold (N=1) unless otherwise specified.

Results:

Aggregates were formed in non-adherent wells after as little as 2 days (Figure 4). These aggregates gradually decreased in size as the culture period continued presumably due to compaction as the cells produce their own ECM. A Live/Dead stain was performed on wells post seeding to ensure that a vast majority of cells put into the model were alive. On day 4 after seeding into the wells, aggregates had an average diameter of 160μm. Calcium could be visualized within the aggregates as early as day 4 and gradually increased over time (5). Based on these finding imaging of aggregates were performed on day 4 after deposits could be visualized, and then at day 7 to visualize the progression after one full week, which was the typical length of a 2D calcification experiment done in our lab.
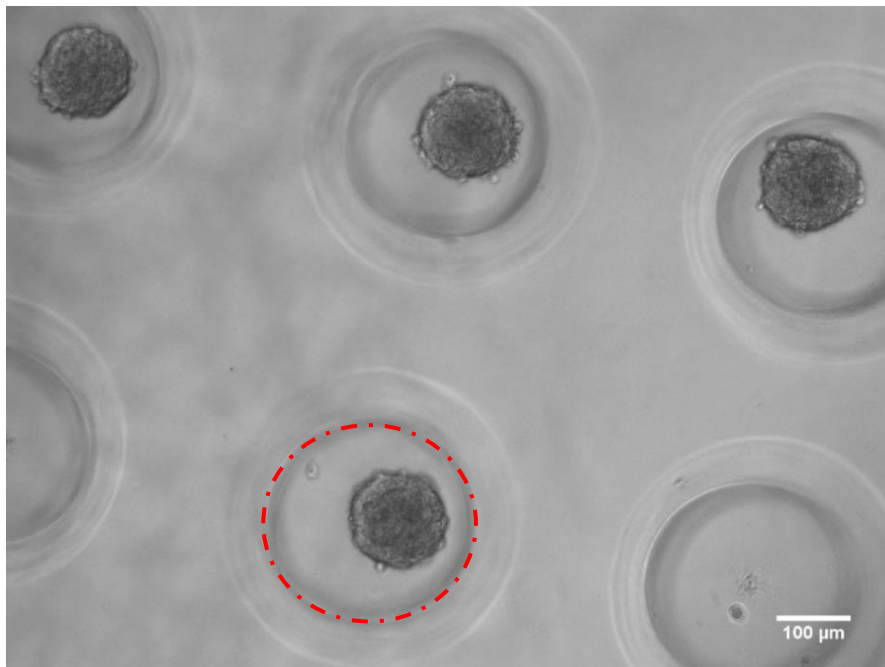

Figure 4 Formed Aggregates: Phase (10x) image of day 2 porcine aortic VIC aggregates formed is non-adherent agarose mold. Each mold is seeded with one million VICs. The red circle indicates the outline of a single well in the mold, with the darker circles being formed aggregates. Scale bar = 100μm
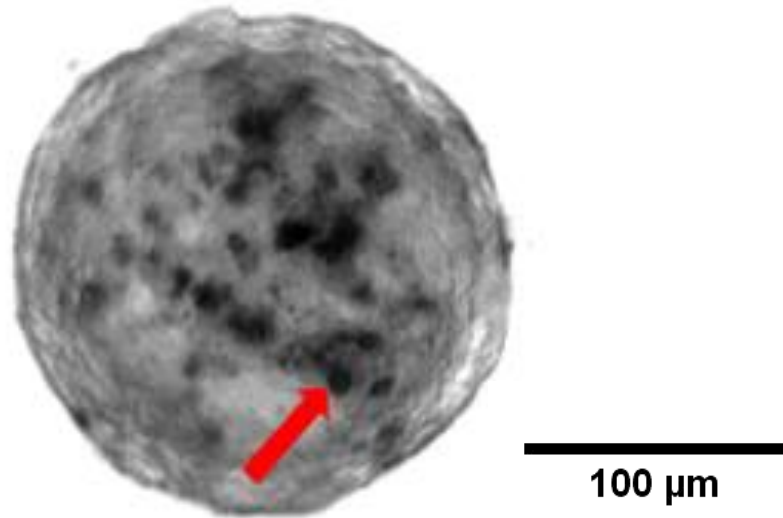
Figure 5 Calcified Aggregate: Phase (20x) image of Von-Kossa stain showing calcification on a day 4 porcine aortic VIC aggregate. Red arrow points to a calcific nodule which become black once stained. Scale bar = 100μm

At times, aggregates merge together to form double and triple aggregates. Within these larger aggregates, multiple cores of calcification and dead cells can be seen. The dual core is clearly observed through both Von-Kossa stains (black, Figure 6) and Live/Dead stains (green/red, Figure 7). This observation points to the importance of the microenvironment within the aggregates as well as ECM composition in determining the health of the cells.
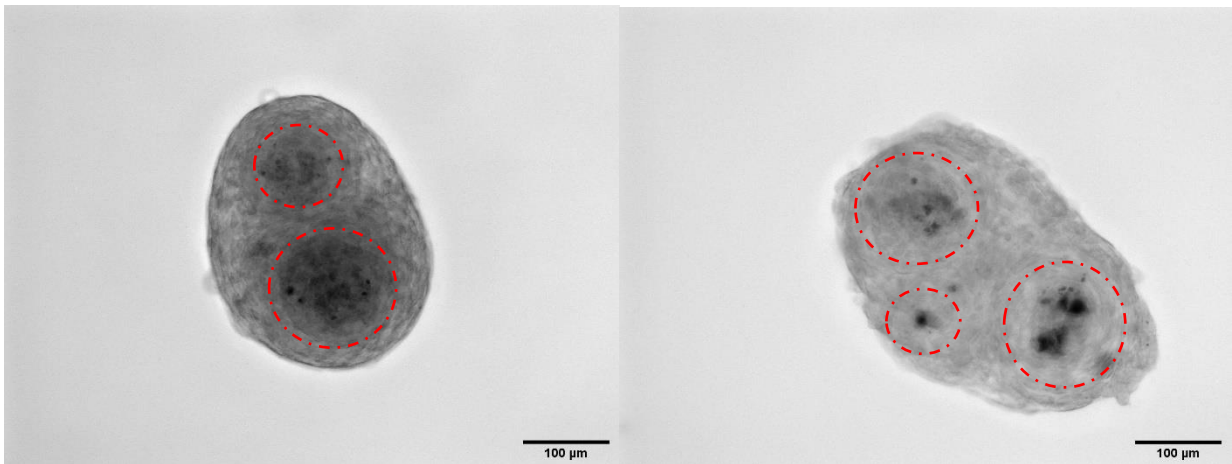

Figure 6 Calcium Stain of Merged Aggregates: Pahe (10x) image of Von-Kossa stain on two (left) and three (right) merged day 4 porcine aortic VIC aggregates. Aggregate formation can still be seen in merged aggregates with the circular cell orientation around calcific nodules in both images. Red circles show where the individual aggregates microenvironment remains within the merged aggregates. Scale bar = 100μm
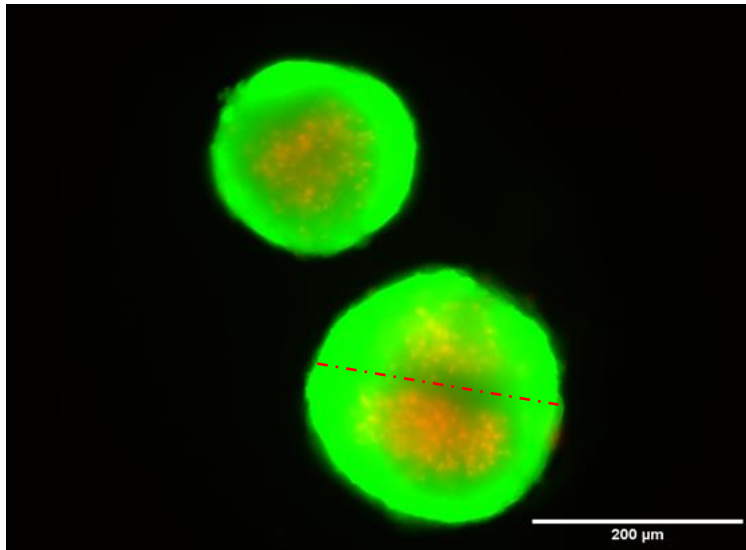
Figure 7 Live/Dead Stained Merged Aggregaate: Live (green)/Dead (red) stain of a singular (top) and two merged day 2 porcine aortic VIC aggregates (bottom). The image reveals a gap in dead cells between the merged aggregates (represented by the red dotted line) where as there is a single core of cell death in the sole aggregate. Scale bar = 200µm

Effect of Ascorbic Acid Supplementation on Aggregates:

To determine if ascorbic acid has the same anti-calcification effects on our cell line as previously observed, aggregates were supplemented with 250µM from day 0. Von Kossa stains revealed that supplementation of AA was in fact able to prevent calcification as seen in Figure 8.
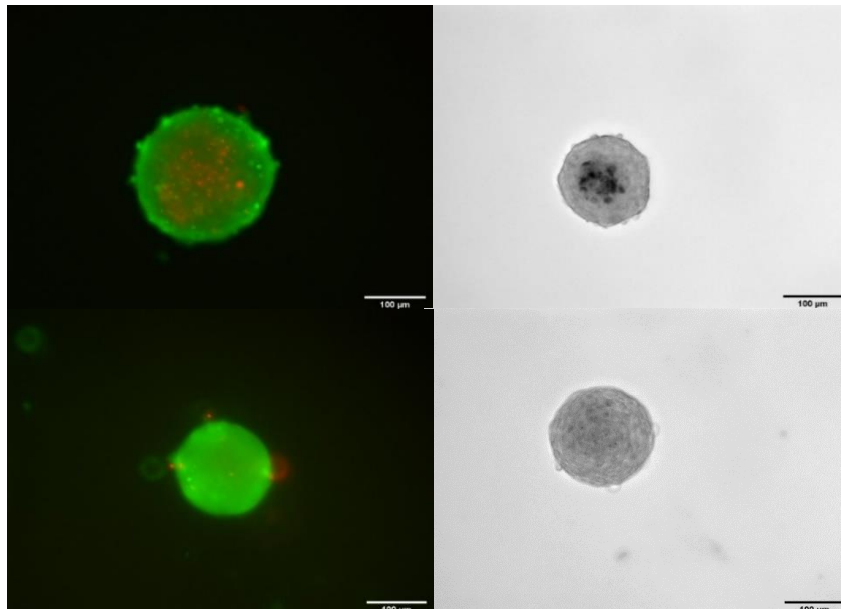

Figure 8 Ascorbic Acid Supplemented Aggregates: Live (green)/Dead (red) stain of passage 7, day 4 porcine aortic VIC aggregates (left) and phase image (10x) of passage 4, day 4 porcine aortic VIC aggregates (right). The top row is the control, and the bottom row are aggregates supplemented with 250µM ascorbic acid. Supplementation of ascorbic acid affectively blocked cell death as well as preventing calcification. Scale bar = 100µm

Cells of the same passage were also stained with Live/Dead showing that AA also prevented cell death which was observed in the center on non-treated aggregates.

Effect of blocking apoptosis with Z-VAD:

To determine if apoptosis is integral to calcification in 3D aggregates as it has been demonstrated in 2D aggregates, apoptosis was blocked using Z-VAD, followed by Von-Kossa stain. Implementation of Z-VAD for 5 days culture in 2D before seeding aggregates in micro-molds resulting in a mean corrected total cell fluorescence per area of 106 ± 46 (Figure 9).
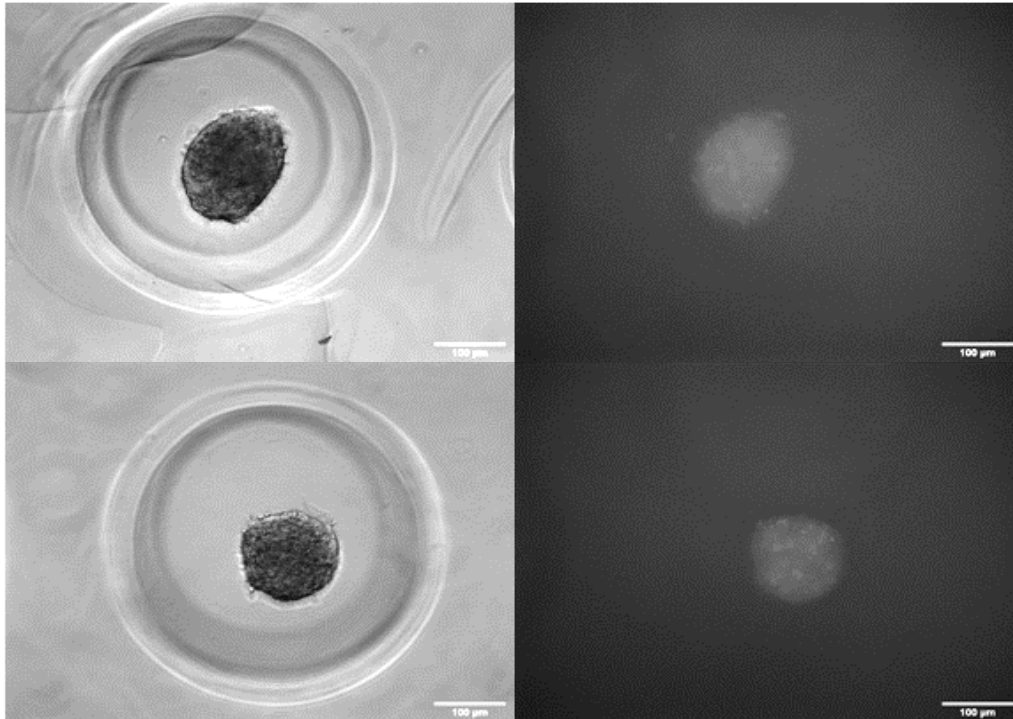

Figure 9 Day 4 Caspase Stain on Z-VAD Supplemented Aggregates: Phase image (10x)(left) and caspase stain (right) on passage 9, day 4 porcine aortic VIC aggregates in mold with caspase inhibitor Z-VAD showing moderate levels of apoptosis even with the inhibitor. Scale bar = 100µm

Previous experiments had shown dense regions of apoptosis centered in the core of aggregates not treated with Z-VAD (Figure 10). The mean corrected total cell fluorescence per area for these aggregates was 937 ± 74. So, while Z-VAD significantly reduces the apoptosis seen in aggregates, it is important to note that there are still spots of apoptosis that occur, resulting in potential nucleation sites for calcium nodule formation.
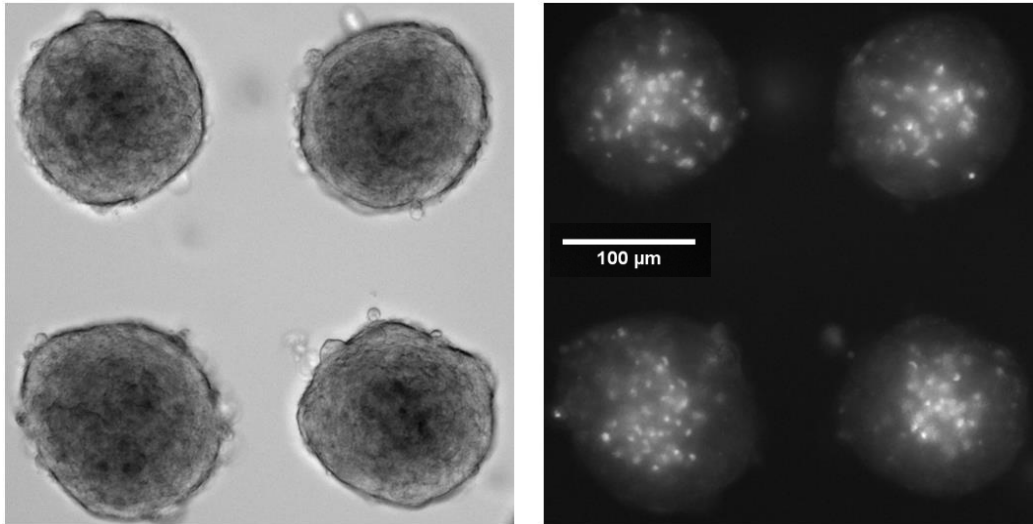
Figure 10 Day 4 Caspase Stain on Control Aggregates: Phase image (20x)(left) and caspase stain (right) on passage 5, day 2 porcine aortic VIC aggregates not treated with Z-VAD or AA showing high levels of apoptosis. Scale bar = 100μm

Performing a Von-Kossa stain on day 4 aggregates with Z-VAD indicates minimal calcification with a few calcium nodules present (Figure 11 (left)). This extent of calcification is noticeably less than calcium formation on non-treated aggregates (Figure 11 (right)).
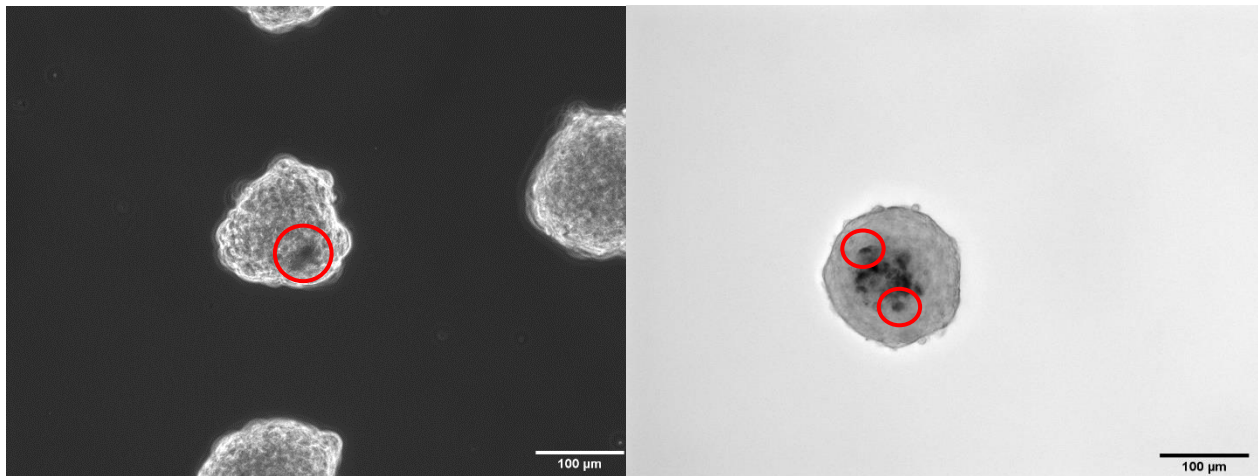

Figure 11 Calcium Stain of Day 4 Z-VAD Supplemented Aggregates: Image (20x, phase) passage 9, day 4 porcine aortic VIC aggregates stained with Von Kossa (left) showing small, calcified region circled in red. This is a significant difference to what can be seen in control passage 4, day 4 porcine aortic VIC aggregates stained with Von Kossa (right, transmitted light) with nodules circled in red. Differences in background are due to a change in microscope technique in later experiments to better visualize nodules. Scale bar = 100μm

By day 7, the apoptosis significantly increases in aggregates treated with Z-VAD with a mean corrected total cell fluorescence per area of 286±62. This would result in increasing nucleation sites for calcium deposits (Figure 2). This overall shows that Z-VAD is effective as a caspase
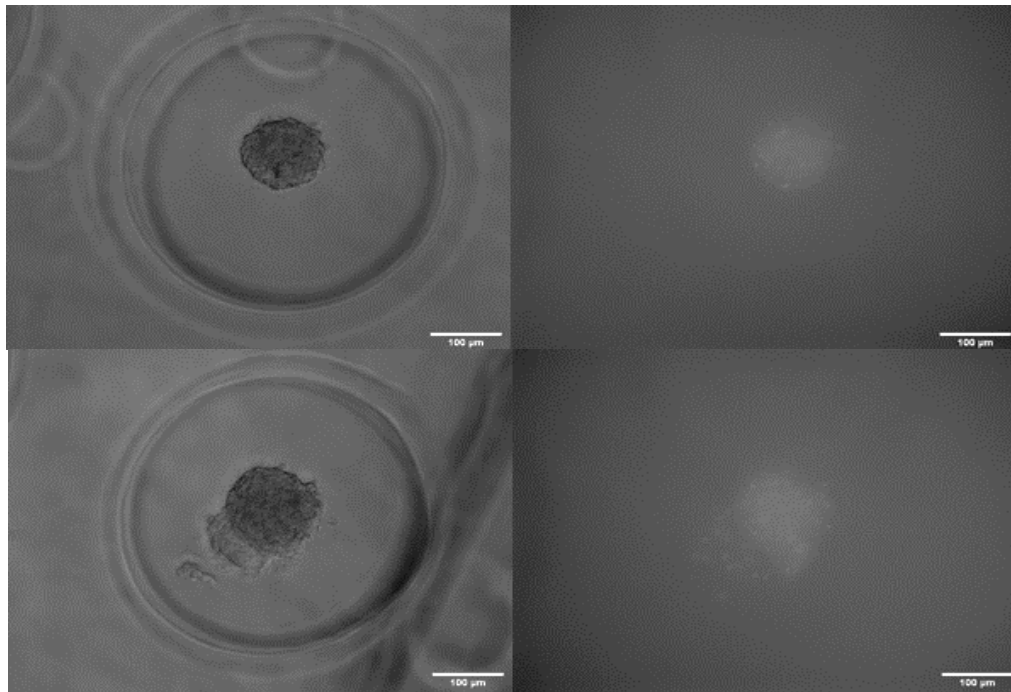

Figure 12 Day 7 Caspase Stain on Z-VAD Supplemented Aggregates: Phase image (10x) (left) and caspase stain (right) on Passage 9 VICs Day 7 with Caspase inhibitor Z-VAD. Scale bar = 100µm

inhibitor in the cell spheroids minimizing, but not fully eliminating, programmed cell death. This inhibitor allowed us to study the importance of apoptosis in calcification and the dystrophic pathway in our model. After 7 days of culture with Z-VAD aggregates showed multiple nucleation sites, but an substantially less calcification than observed in non-treated aggregates (Figure 13). Due to Z-VAD not entirely blocking apoptosis, nucleation sites still form. Over the course of seven days this gradual slow apoptosis may build up on those sites resulting in calcific spots seen in Figure 14.
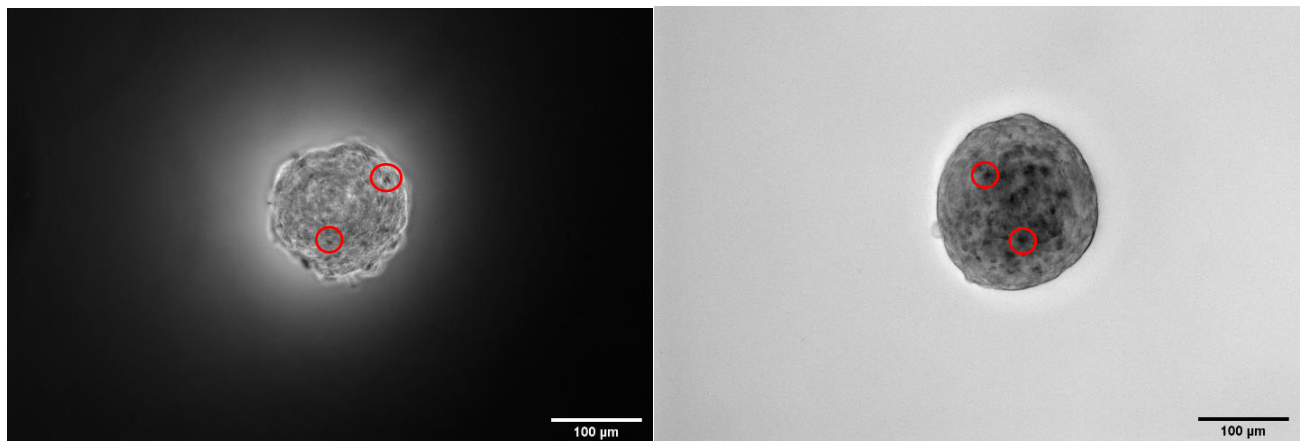
Figure 83 Calcium Stain of Day 7 Z-VAD Supplemented Aggregates: Image (20x, phase) passage 9, day 7 porcine aortic VIC aggregates stained with Von Kossa (left) showing small, calcified region circled in red. This is a significant difference to what can be seen in control passage 4, day 7 porcine aortic VIC aggregate (right, transmitted light). Differences in background are due to a change in microscope technique in later experiments to better visualize nodules. Scale bar = 100µm

Inducing oxidative stress with H_2O_2:

      To help understand the role of oxidative stress on the 3D aggregates, two separate antioxidants were chosen to be tested in addition to ascorbic acid, Trolox and methionine. The cells were treated with the antioxidants and then the media was supplemented with hydrogen peroxide to induce stress. Live/Dead stains were performed to determine the effectiveness of the antioxidants and varying concentration against the induced stress (Figure 94). In the 2D monolayer tests, it was determined that the ideal concentrations of H_2O_2 in DMEM for the purpose of this study were 250μM and 500μM, as this provided clear effects of the induced oxidative stress without it killing a majority of the cells.
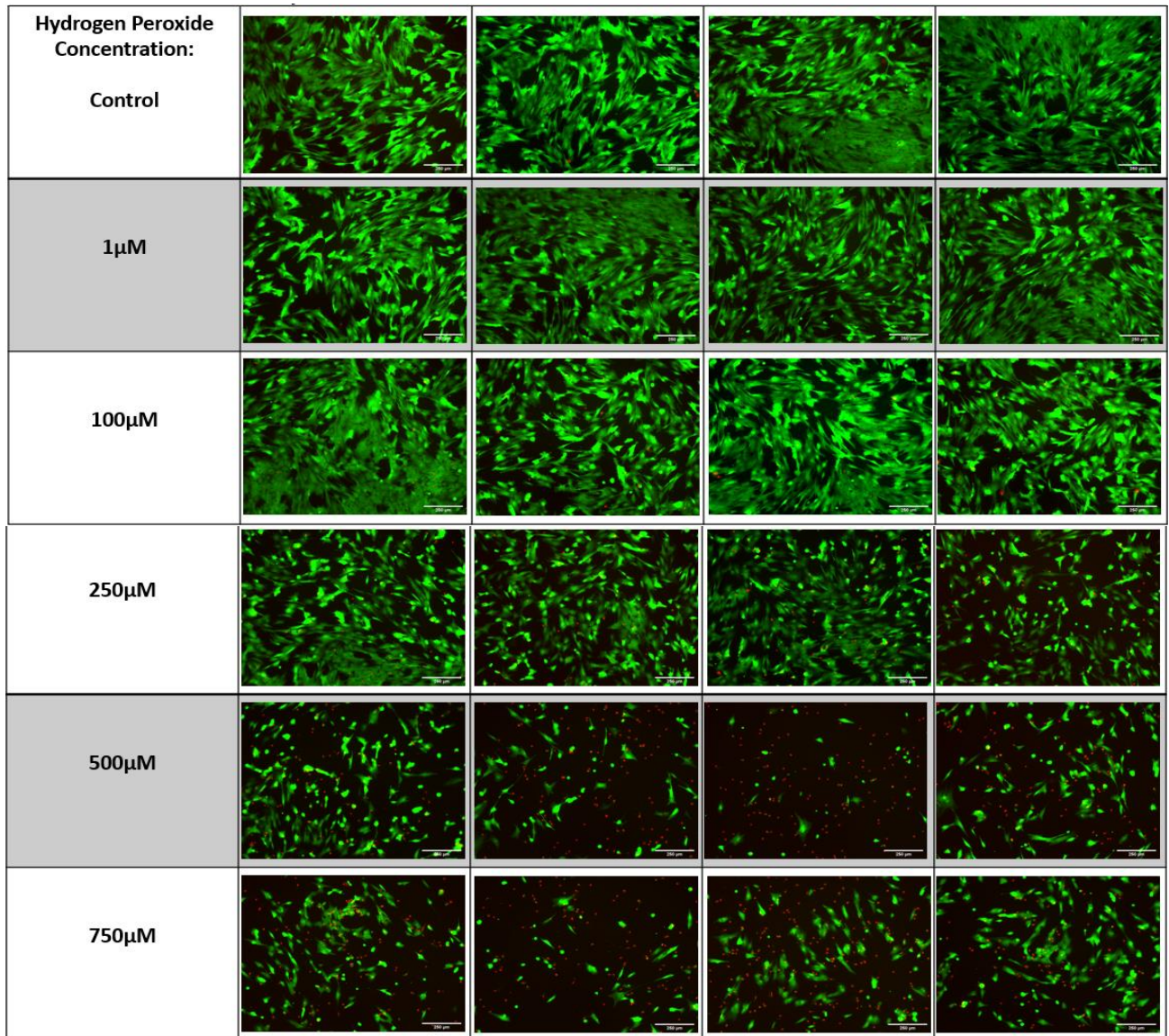

Figure 94 Stressing VICs in 2D with Hydrogen Peroxide: Determining Hydrogen Peroxide concentration to induce stress to PAVICs using Live(green)/Dead(red) stain. Each row represents four replicates at each concentration (n=4). Between 250μM and 500μM was where a large increase in dead cells was seen without killing a majority of the cells. Scale bar = 100μm

Determination of antioxidant efficacy in 2D culture:

The concentrations of H_2O_2 determined in the previous experiment was then used on cells in a monolayer that were pretreated with ascorbic acid, Trolox, and methionine 24 hours. H_2O_2 was added for 24 hours and alamarBlue™ added for the final 8 hours. This resulted in an alamarBlue™ signal as a value which showed ascorbic acid and Trolox fully protecting against the induced oxidative stress at 250μM and 500μM, respectively (Figure 15). Methionine was able to offer some protection of the induced stress at both tested concentrations but was most protective at 200μM. This provided enough evidence to these antioxidants provide significant protection against oxidative stress to be used on the 3D aggregate model.
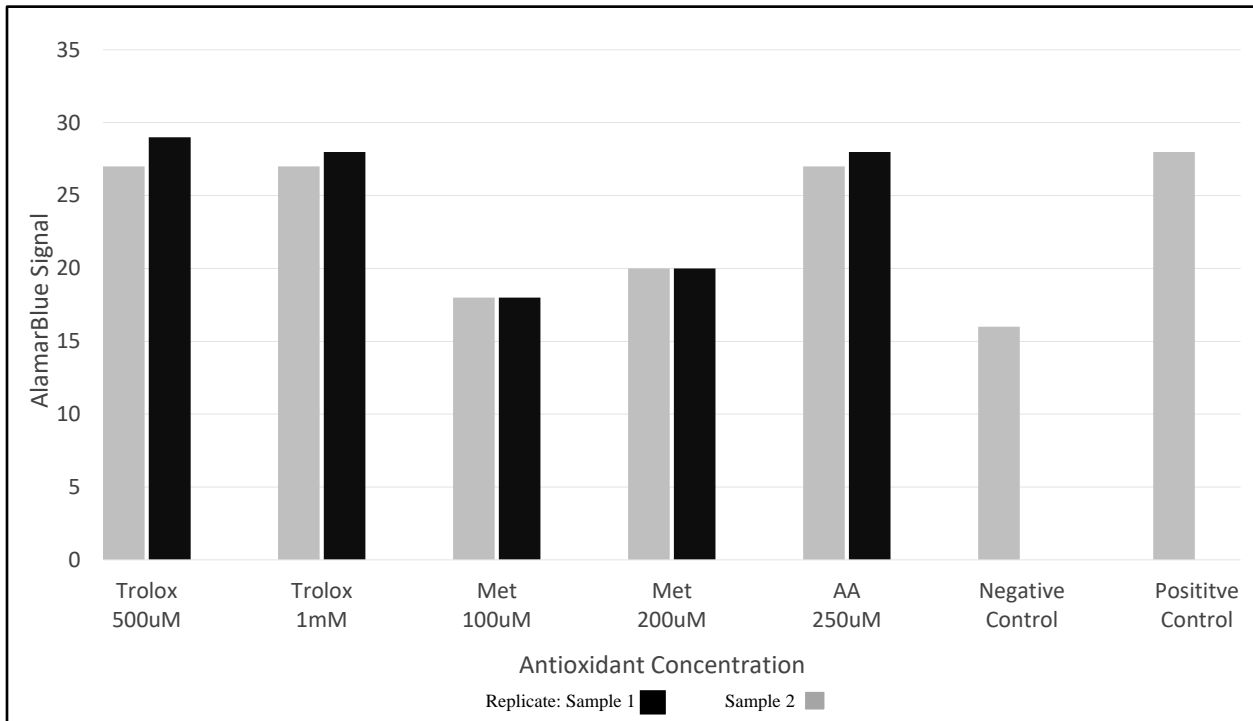

Figure 105 AlamarBlue™ Results: AlamarBlue™ signal revealing cell viability after hydrogen peroxide-induced stress on two replicates (n=2). Results show that a Trolox concentration of 500μM and ascorbic acid concentration of 250μM protected the cells against the induced stress. Methionine provided some protection against induced stress with the most protection at a concentration of 200μM. Negative control is H_2O_2 without any antioxidant and positive control is no H_2O_2.

Antioxidant effect in 3D aggregates:

After determining effective concentrations of the antioxidants to protect against H2O2-induced oxidative stress, they were supplemented in the media fed to aggregates from day 1 of culture. On day 4 Von-Kossa stains showed that calcification was significantly reduced in aggregates treated with the AA and Trolox compared to the control (Figure 16). Image analysis reveals that AA and Trolox had 0.07%±0.05 and 0.7%±0.5 area calcified, respectively. Compared to the control, which had 3.01%±1.5 calcification, this was a significant decrease. Methionine also had a slight reduction in calcification buildup at 1.6%±0.8. This is believed to be due to the ability of the antioxidants to protect against oxidative stress and therefore reduce apoptosis occurring.
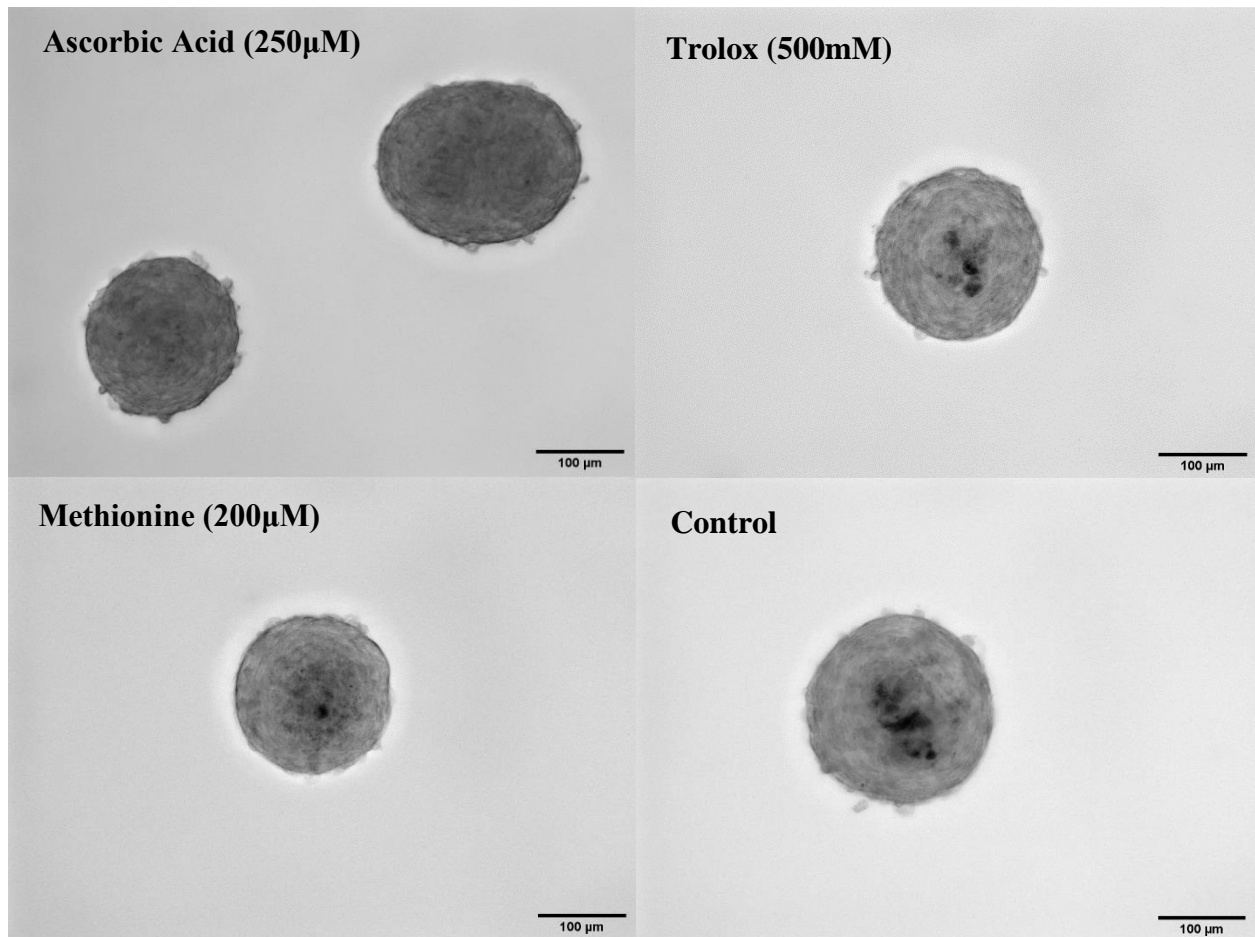
Figure 16 Calcium Stain on Antioxidant Supplemented Day 4 Aggregates: Images (20x) of porcine aortic VIC aggregates Day 4 Passage 4 with Von-Kossa stain for various antioxidant treatments. Scale bar = 100µm

By day 7 Von-Kossa staining revealed that the calcification progressed similarly to how it was seen on day 4 (Figure 17). At this timepoint, however, the calcification buildup in Trolox had become much more prevalent at 2.5%$\pm$0.8, while AA was still able to prevent calcium buildup nearly completely at 0.2%$\pm$0.2. Both were significantly less than the control, which had 7.7%$\pm$1.9 of its total area as calcium Methionine had a large calcium buildup in the core of the aggregate, resulting in 6.0%$\pm$1.9, but once again was slightly less than the control. This points to the potential of multiple factors playing a role in the calcium formation. If the protection against oxidative stress was the only inducer of dystrophic calcification, then it would be expected that Trolox would prevent calcification to the same extent as AA. The overall results of the PCPA can be seen below in Figure 18. Aggregates on day 4 and 7 were also measure for total area to see if there were any significant differences in size depending on which antioxidant was supplemented. Results showed no major differences across area of aggregates of the same day and shows a small reduction in area between day 4 and 7. This revealed that in this experiment calcification did not affect the size of aggregates, which is believed to be due to aggregates forming ECM and therefore the general size before calcification occurs.
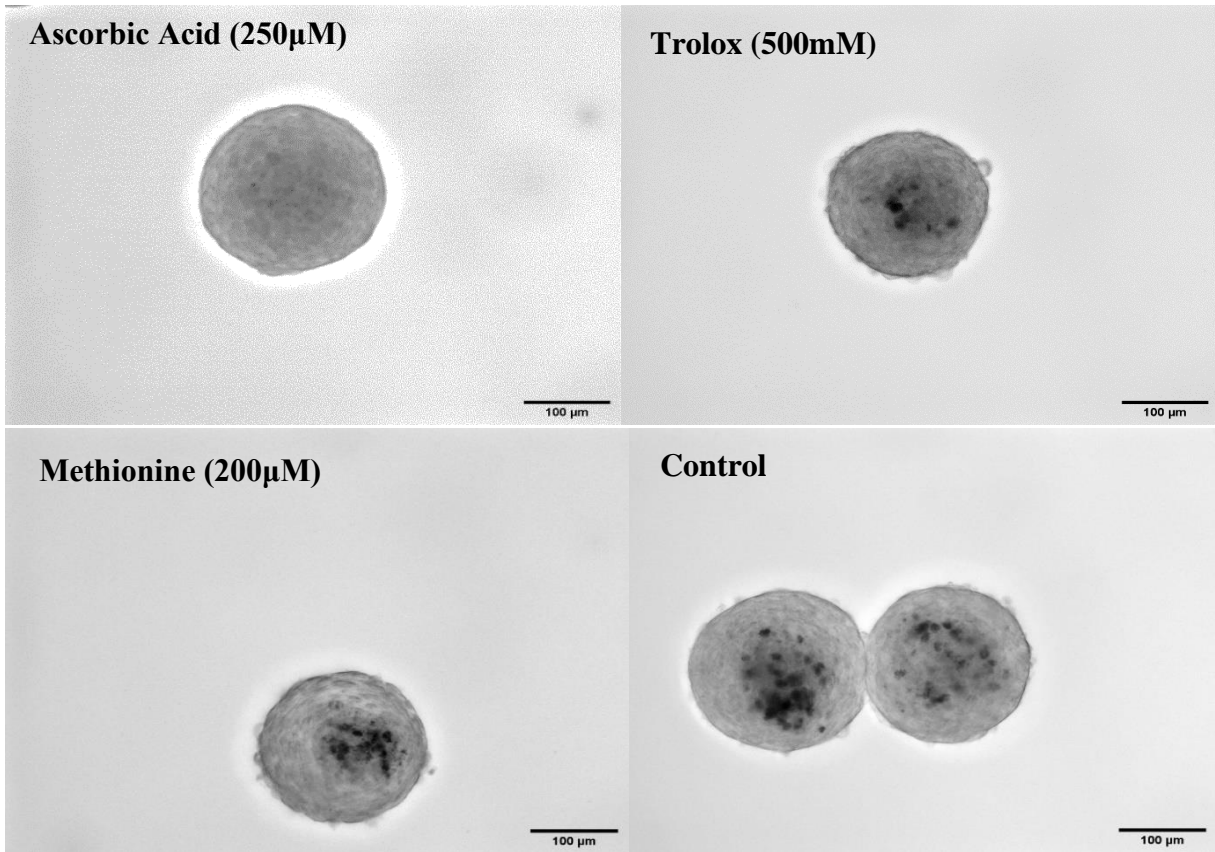
Figure 17 Calcium Stain on Antioxidant Supplemented Day 7 Aggregates: Phase image (20x) of porcine aortic VIC aggregates Day 7 Passage 4 with Von-Kossa stain for various antioxidant treatments. Scale bar = 100μm

Figure 18 Antioxidant Experiment Results: Percent calcification per total area of aggregates treated with different antioxidants (AA 250μM, Trolox 500μM, Methionine 200μM) on day 4 and 7. Asterix (*) represent significant difference from the control group (H2O2 treated, no antioxidants). Double Asterix (**) represents significant difference from AA.

Discussion:

One of the major gaps within research on CAVD comes from the abundance of 3D models using osteogenic means to induce calcification rather than the more common dystrophic. The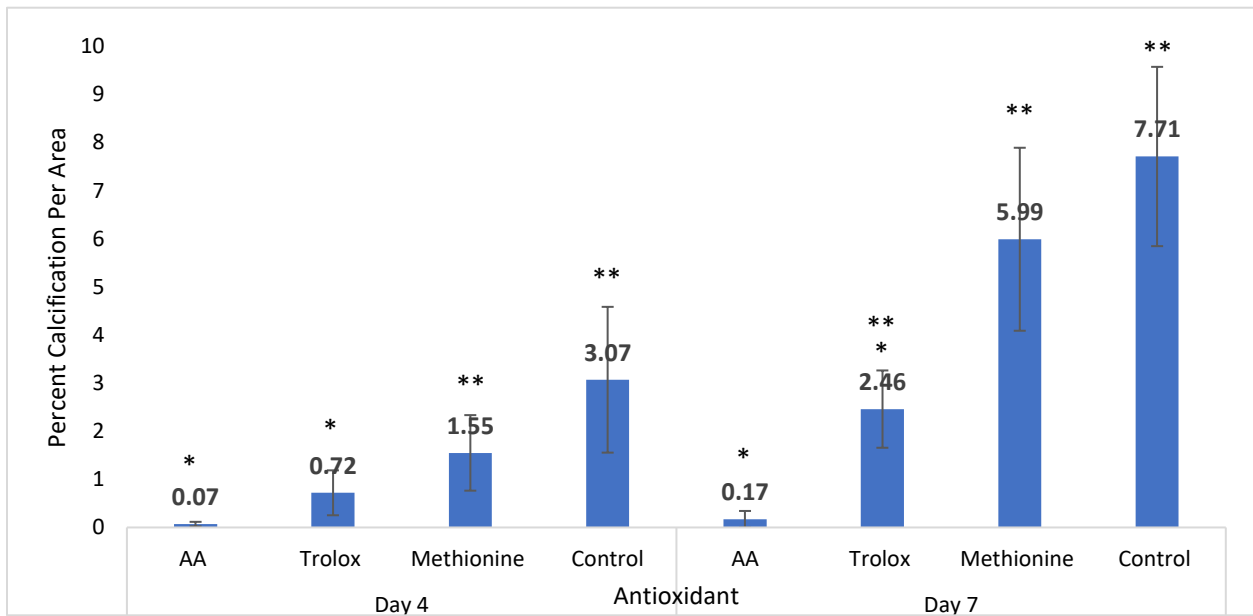refore, there was a need for a 3D model that could be used to further understand the mechanisms of dystrophic calcification. With the method of forming aggregates from Roosens et al. which consistently produces calcific nodules, we had a platform to test potential calcium inducing factors. Roosens et al. also was able to find a way to consistently prevent any calcium buildup in aggregates using ascorbic acid. While Roosens et al. was using the aggregates as building blocks for the bio-fabrication of heart valve tissue, it provides a potentially powerful model to gain better insight on the mechanisms of calcification. The benefit of using such a model instead of single cells or aggregates which spontaneously calcify by encapsulating them in a hydrogel, the influence of substrate modulus on VIC phenotype and calcification can be known. While there are numerous possible mechanisms involved in the dystrophic pathway, here we studied two specific factors: apoptosis and oxidative stress. As seen in 2D model systems, apoptosis is an integral part of the calcification pathway, but this has yet to be further shown in 3D. Antioxidants and their protective properties against oxidative stress has also been an area of interest, especially with this model as ascorbic acid was able to completely prevent calcification in 3D aggregates. Incorporating these in our 3D model allowed us to recapitulate and confirm that apoptosis as well as antioxidants do play a significant role in calcification. This allowed us to reach our goal of better understanding the dystrophic pathway and point to potential therapeutic targets as wells as point where research should continue.

One of the well-studied parts of the dystrophic pathway in 2D models is programmed cell death. One study by Proudfoot et al. revealed that apoptosis occurred prior to the onset of calcification, and apoptotic bodies could produce calcium in a crystallized form [24]. A later experiment by the same group found that the inhibition of apoptosis with the caspase inhibitor Z-VAD was capable of reducing calcification nodules by roughly 40% [25]. This was recapitulated by Fisher et al. again found that through using Z-VAD to block apoptosis, there was an significant reduction in the number of calcific nodules [5]. This was further shown in porcine aortic VICs using another means of inhibiting apoptosis, M50054, which also significantly decreased calcium nodule formation [26]. To see if increasing programed cell death would produce the opposite result, Proudfoot et al. stimulated apoptosis in nodular cultures using anti-Fas IgM, and found that there was a 10-fold increase in calcification [24]. Fujita et al took a different approach where they added dead cells to the culture and found that necrotic areas of dead cells became surrounded by calcium deposits [27]. Mathieu et al found that apoptotic bodies derived from plasma membrane are rich in ectonucleotidases and promote the nucleation and formation of spheroid mineralized microparticles, which are the basic unit of mineralized material formed in CAVD [28]. Further, Galeone et al. demonstrated that the pro-apoptotic cytokine TRAIL is found to be expressed in human calcified aortic valves but not in normal healthy ones [29]. With numerous studies showing the importance of programmed cell death in the formation of calcium nodules, we decided to incorporate similar studies to see if this finding would be recapitulated in 3D. While these studies were performed in 2D or through studying human valves, we wanted to see how blocking apoptosis would affect the calcification that was

consistently shown in our 3D aggregate model. By blocking apoptosis through a caspase inhibitor Z-VAD, we found a great reduction in the calcium formation. While Z-VAD was effective at significantly reducing the amount of apoptosis occurring in the aggregates it was not able to completely prevent it, while we believe completely bocking apoptosis could have had an even stronger effect of reducing or even completely blocking calcification.

Another important focus of research on CAVD has been on the role of the ECM on valvular calcification. While this research had similar limitations around it primarily using osteogenic conditions to study the calcium buildup, there are still major takeaways that could apply to dystrophic calcification. There have been several groups that show specific ECM compositions or culture substrates plays a crucial role in calcification. For example, VICs cultured on collagen and fibronectin were resistant to calcification, even upon treatment with mineralization-inducing growth factors such as BMPs and TGF-β1 [30]. This implies that collagen and fibronectin are actively performing functions that inhibit VIC calcification having similar effects at preventing calcification as ascorbic acid [30]. Ascorbic acid has also been shown to be essential for collagen biosynthesis which points to this as a contribution to its ability to prevent calcification in our 3D aggregate model [31]. These finding of ECM components playing a key role in calcification has also been seen through heart valves of patients who had CAVD. Hutson et al. found that CAVD is associated with layer-specific alterations in collagen architecture and specifically points to the disorganization of the valve ECM as a hallmark of CAVD [32]. They were able to conduct a quantitative, layer-specific characterization of individual collagen fibers in both diseased and healthy human aortic valves, and were able to demonstrate differences in the distribution and architecture of collagen in CAVD [32]. Fondard et al. also found that alterations of the ECM, with a focus on the disorganization of collagen bundles and the fragmentation of elastic fibers was significantly higher in aortic stenosis and aortic regurgitation when compared with controls [33]. Interestingly, they pointed to a contributor of the disorganization of collagen bundles in the fibrosa was due to the presence of calcified nodules, which could mean the ECM was being reorganized due to calcium nodules forming [33]. Due to multiple studies revealing a correlation between collagen and calcification, Eriksen et al. performed an analysis of explanted calcified valves, where they found that total collagen content in valves with CAVD was significantly lower than that found in normal valves [34]. These findings indicate that, during calcification, degradation of collagen exceeds its synthesis. To test this finding, Rodriguez et al. performed the partial removal of collagen from porcine leaflets, and found that doing so was effective at inducing both VIC proliferation and apoptosis relative to non-depleted leaflets, which remained relatively quiescent [35]. Ascorbic acid has also been shown to be essential for collagen biosynthesis [31]. Roosens et al. also did point out that AA acts as a cofactor for post-translational processing enzymes where some participate in collagen hydroxylation [15]. These studies show an important correlation between ECM components with specific focus on collagen, yet the mechanisms are still yet to be elucidated.

While we did not specifically look at the effect of ECM reorganization, our aggregates did show an importance of the ECM in the calcification formation. Specifically, through the images of merged aggregates where two or more aggregates, it is still possible to see the

individual cores. These smaller cores within in the merged aggregates was the primary areas for cell death as well as calcification. Even though these aggregates are larger than typical single aggregates, the lack of cell death in the core leads us to believe that the cause of the death is due to microenvironmental factors that are seen when the VICs have specific circular aggregate cell orientation. This along with previous experiments with apoptosis excludes theories of necrosis in the core of aggregates being the cause of nucleation sites for calcium.

The final and major focus of this study revolved around the role of oxidative stress and antioxidants in the dystrophic pathway. Many different cardiovascular disorders and diseases have been associated with a state of oxidative stress where the expression levels of reactive oxygen species (ROS)-producing enzyme are up-regulated [36]. In these diseases, which includes endothelial dysfunction, hypertension, and cardiac remodeling as well as others, also have the activity and expression of antioxidant mechanisms down-regulated [36]. This has similarly been seen in stages of CAVD where a study was done to assess the oxidative modification of plasma proteins, and found elevated oxidative stress was observed to have correlation with the severity of aortic stenosis (AS) [37]. Recent studies have supported the concept that reactive oxygen species (ROS), which is likely produced by inflammation, plays an important role in the development of the early cellular and extracellular changes associated with aortic valve stenosis [38]. Miller et al. found that in explanted valves from patients with established aortic stenosis, superoxide and H_2O_2 levels were significantly increased in the valve near calcified regions [39]. This finding supports our selection of antioxidants to test as they were shown to have protective effects against oxidative stress induced through H_2O_2. Through researching the effects of a known antioxidant, ellagic acid, Jordão et al. found that administering ellagic acid in rat aorta resulted in less aortic wall thickening and less calcification [40]. They concluded that ellagic acid attenuates hypertension, which possibly improves nitric oxide bioavailability and therefore reducing oxidative stress [40]. Another group using aortic grafts from rats found that there was a correlation between the extent of antioxidant activity, oxidative tissue damage, and calcification that was found in vascular grafts [41]. Based on many of these findings our group aimed to determine if there is a correlation between antioxidant protection against ROS and calcification in our 3D model. We found that supplementation in culture media from day 0 of aggregate formation had a direct impact on the amount of calcium buildup. While AA was effective at completely preventing calcium, Trolox and methionine were both able to significantly reduce the percent calcium per area compared to the control. While it is presumed that antioxidant properties alone may not be enough to prevent calcium, they reveal a promising avenue for therapeutic research. Unfortunately, despite this strong evidence that ROS are involved in CAVD, oral antioxidant treatments in atherosclerosis have been largely unsuccessful [42].

Through these experiments we were able to show that these aggregates model dystrophic calcification and is therefore a viable model to study CAVD. In comparison to in-vivo calcification this model as well as other 2D models in literature calcify significantly faster than typically seen through the progression of the disease in a valve. This was also on par for the rate of calcification seen through the study by Roosen et al. where they could visual calcium deposits after three days [15]. This is expected to be due to the forced aggregation of a large mass of cells

which will activate the VICs initiating the dystrophic pathway. One advantage of this accelerated process is how it is a faster method for studying the effect of different compounds on the calcification. This overall helps the model provide a good means to perform early stages of clinical studies in regard to calcification. There would need to be further research done on the impact of antioxidants on calcification however which would need to shift to in vivo studies, as this model is both accelerated, and missing mechanical stresses which could impact the calcification pathway.

Overall, this study was able to recapitulate previous 2D studies revealing apoptosis is also integral is calcification in 3D. We were also able to show a correlation between calcium formation and oxidative stress through the use of antioxidant supplementation to aggregate culture medium. Through imaging of merged aggregates during culture we were also able to show a direct correlation between the microenvironment of the aggregates as the calcium deposits are only present in the center of a formed aggregate. These findings lead us to believe that calcification is the result of multiple factors including oxidative stress as well as cell-interaction with extracellular matrix components (or lack thereof). One possible explanation of this pathway could be that oxidative stress leads to remodeling of aortic valves, causing changes in the ECM which lead to apoptosis, and thus results in calcium nucleation sites which build up over time. While this leaves a lot to be learned about CAVD, it points researchers in directions which should be focused on to better understand the dystrophic pathway and potential therapeutic options.

Future Recommendations

Future studies are needed to examine the role of the ECM within aggregates and how it affects calcium nodule formation. Since AA and Trolox maintained cell viability despite induced oxidative stress, but only AA was able to fully prevent any calcium buildup, it would be beneficial to determine the ECM composition of those aggregates. Comparing this with the ECM of controls as well as Methionine, which had some prevention of calcification, could provide insight as to what specific components have calcium preventative capabilities. Focusing on specific ECM components could also be beneficial, with specific focus recommended for collagen, which is a major component of heart valve ECM. Supplementation of aggregates with collagen could be done to see the impact on calcium buildup. Another possible study would be to reintroduce the ECM of aggregates supplemented with AA. Doing so could be useful for determining if the main preventative qualities of AA in calcium buildup come from its effect on the ECM or rather its antioxidant properties. It could also be beneficial to co-stain aggregates and image using a confocal microscope to characterize co-localization of regions of calcification, apoptosis, and collagen. To gain further insight on merged aggregates we would recommend performing an experiment to determine when and under what specific conditions aggregates will merge, and then being able to image them at different timepoints post merging. Lastly, to better mimic an in vivo environment, aggregates should be seeded into a stretchable model to incorporate mechanical stresses.

Funding

Disclosure of conflict of interest:

None.

References:

1. Lerman, D.A., S. Prasad, and N. Alotti, *Calcific Aortic Valve Disease: Molecular Mechanisms and Therapeutic Approaches.* Eur Cardiol, 2015. **10**(2): p. 108-112.
2. Yutzey, K.E., et al., *Calcific aortic valve disease: a consensus summary from the Alliance of Investigators on Calcific Aortic Valve Disease.* Arterioscler Thromb Vasc Biol, 2014. **34**(11): p. 2387-93.
3. Desai, C.S., et al., *Transcatheter aortic valve replacement: current status and future directions.* Semin Thorac Cardiovasc Surg, 2013. **25**(3): p. 193-6.
4. Mohler, E.R., 3rd, et al., *Bone formation and inflammation in cardiac valves.* Circulation, 2001. **103**(11): p. 1522-8.
5. Fisher, C.I., J. Chen, and W.D. Merryman, *Calcific nodule morphogenesis by heart valve interstitial cells is strain dependent.* Biomech Model Mechanobiol, 2013. **12**(1): p. 5-17.
6. Walker, G.A., et al., *Valvular myofibroblast activation by transforming growth factor-beta: implications for pathological extracellular matrix remodeling in heart valve disease.* Circ Res, 2004. **95**(3): p. 253-60.
7. Yip, C.Y., et al., *Calcification by valve interstitial cells is regulated by the stiffness of the extracellular matrix.* Arterioscler Thromb Vasc Biol, 2009. **29**(6): p. 936-42.
8. Cirka, H.A., et al., *Reproducible in vitro model for dystrophic calcification of cardiac valvular interstitial cells: insights into the mechanisms of calcific aortic valvular disease.* Lab Chip, 2017. **17**(5): p. 814-829.
9. Duan, B., et al., *Active tissue stiffness modulation controls valve interstitial cell phenotype and osteogenic potential in 3D culture.* Acta Biomater, 2016. **36**: p. 42-54.
10. Hjorntaes, J., et al., *Simulation of Early Calcific Aortic Valve Disease in a 3D Platform: A Role For Myofibroblast Differentiation*. 2016: Journal or Molecular and Cellular Cardiology. p. 13-20.
11. Monroe, M.N., R.C. Nikonowicz, and K.J. Grande-Allen, *Heterogeneous multi-laminar tissue constructs as a platform to evaluate aortic valve matrix-dependent pathogenicity.* Acta Biomater, 2019. **97**: p. 420-427.
12. Butcher, J.T. and R.M. Nerem, *Porcine aortic valve interstitial cells in three-dimensional culture: comparison of phenotype with aortic smooth muscle cells.* J Heart Valve Dis, 2004. **13**(3): p. 478-85; discussion 485-6.
13. Mabry, K.M., R.L. Lawrence, and K.S. Anseth, *Dynamic stiffening of poly(ethylene glycol)-based hydrogels to direct valvular interstitial cell phenotype in a three-dimensional environment.* Biomaterials, 2015. **49**: p. 47-56.
14. Zabirnyk, A., et al., *A Novel Ex Vivo Model of Aortic Valve Calcification. A Preliminary Report.* Front Pharmacol, 2020. **11**: p. 568764.
15. Roosens, A., I. Puype, and R. Cornelissen, *Scaffold-free high throughput generation of quiescent valvular microtissues.* J Mol Cell Cardiol, 2017. **106**: p. 45-54.

16.   Zeisel, S.H., *Antioxidants suppress apoptosis.* J Nutr, 2004. **134**(11): p. 3179S-3180S.

17.   Gould, R.A. and J.T. Butcher, *Isolation of valvular endothelial cells.* J Vis Exp, 2010(46).

18.   Deegan, A.J., et al., *A facile in vitro model to study rapid mineralization in bone tissues.* Biomed Eng Online, 2014. **13**: p. 136.

19.   Rampersad, S.N., *Multiple applications of Alamar Blue as an indicator of metabolic function and cellular health in cell viability bioassays.* Sensors (Basel), 2012. **12**(9): p. 12347-60.

20.   Walsh, J.G., et al., *Executioner caspase-3 and caspase-7 are functionally distinct proteases.* Proc Natl Acad Sci U S A, 2008. **105**(35): p. 12815-9.

21.   Pienkowska, N., et al., *Effect of antioxidants on the H2O2-induced premature senescence of human fibroblasts.* Aging (Albany NY), 2020. **12**(2): p. 1910-1927.

22.   Koziel, R., et al., *Methionine restriction slows down senescence in human diploid fibroblasts.* Aging Cell, 2014. **13**(6): p. 1038-48.

23.   Gibson, G.E., et al., *Differential alterations in antioxidant capacity in cells from Alzheimer patients.* Biochim Biophys Acta, 2000. **1502**(3): p. 319-29.

24.   Proudfoot, D., et al., *The role of apoptosis in the initiation of vascular calcification.* Z Kardiol, 2001. **90 Suppl 3**: p. 43-6.

25.   Proudfoot, D., et al., *Apoptosis regulates human vascular calcification in vitro: evidence for initiation of vascular calcification by apoptotic bodies.* Circ Res, 2000. **87**(11): p. 1055-62.

26.   Gu, X. and K.S. Masters, *Role of the MAPK/ERK pathway in valvular interstitial cell calcification.* Am J Physiol Heart Circ Physiol, 2009. **296**(6): p. H1748-57.

27.   Fujita, H., et al., *Necrotic and apoptotic cells serve as nuclei for calcification on osteoblastic differentiation of human mesenchymal stem cells in vitro.* Cell Biochem Funct, 2014. **32**(1): p. 77-86.

28.   Mathieu, P., R. Bouchareb, and M.C. Boulanger, *Innate and Adaptive Immunity in Calcific Aortic Valve Disease.* J Immunol Res, 2015. **2015**: p. 851945.

29.   Galeone, A., et al., *Aortic valvular interstitial cells apoptosis and calcification are mediated by TNF-related apoptosis-inducing ligand.* Int J Cardiol, 2013. **169**(4): p. 296-304.

30.   Rodriguez, K.J. and K.S. Masters, *Regulation of valvular interstitial cell calcification by components of the extracellular matrix.* J Biomed Mater Res A, 2009. **90**(4): p. 1043-53.

31.   Pinnell, S.R., *Regulation of collagen biosynthesis by ascorbic acid: a review.* Yale J Biol Med, 1985. **58**(6): p. 553-9.

32.   Hutson, H.N., et al., *Calcific Aortic Valve Disease Is Associated with Layer-Specific Alterations in Collagen Architecture.* PLoS One, 2016. **11**(9): p. e0163858.

33.   Fondard, O., et al., *Extracellular matrix remodelling in human aortic valve disease: the role of matrix metalloproteinases and their tissue inhibitors.* Eur Heart J, 2005. **26**(13): p. 1333-41.

34.   Eriksen, H.A., et al., *Type I and type III collagen synthesis and composition in the valve matrix in aortic valve stenosis.* Atherosclerosis, 2006. **189**(1): p. 91-8.

35.   Rodriguez, K.J., et al., *Manipulation of valve composition to elucidate the role of collagen in aortic valve calcification.* BMC Cardiovasc Disord, 2014. **14**: p. 29.

36.   Panth, N., K.R. Paudel, and K. Parajuli, *Reactive Oxygen Species: A Key Hallmark of Cardiovascular Disease.* Adv Med, 2016. **2016**: p. 9152732.

37.   Greenberg, H.Z.E., et al., *Role of oxidative stress in calcific aortic valve disease and its therapeutic implications.* Cardiovasc Res, 2021.

38.   Branchetti, E., et al., *Antioxidant enzymes reduce DNA damage and early activation of valvular interstitial cells in aortic valve sclerosis.* Arterioscler Thromb Vasc Biol, 2013. **33**(2): p. e66-74.

39.   Miller, J.D., et al., *Dysregulation of antioxidant mechanisms contributes to increased oxidative stress in calcific aortic valvular stenosis in humans.* J Am Coll Cardiol, 2008. **52**(10): p. 843-50.

40.   Jordao, J.B.R., et al., *Protective Effects of Ellagic Acid on Cardiovascular Injuries Caused by Hypertension in Rats.* Planta Med, 2017. **83**(10): p. 830-836.

41.   Jiang, B., et al., *Vascular scaffolds with enhanced antioxidant activity inhibit graft calcification.* Biomaterials, 2017. **144**: p. 166-175.

42.   Levonen, A.L., et al., *Antioxidant gene therapy for cardiovascular disease: current status and future perspectives.* Circulation, 2008. **117**(16): p. 2142-50.

43.   National Center for Biotechnology Information (2021). PubChem Compound Summary for CID 40634, Trolox. Retrieved August 10, 2021

44.   National Center for Biotechnology Information (2021). PubChem Compound Summary for CID 54670067, Ascorbic acid. Retrieved August 10, 2021

45.   National Center for Biotechnology Information (2021). PubChem Compound Summary for CID 6137, Methionine. Retrieved August 10, 2021

Appendix:

Table A1: Antioxidant and concentration (top) and alamarBlue™ signal (bottom) showing cellular viability to determine effectiveness of antioxidants protection of PAVICs against H2O2 induced stress.

250uM H$_2$O$_2$				500uM H$_2$O$_2$			
Trolox 500uM	Trolox 500uM	Trolox 1mM	Trolox 1mM	Trolox 500uM	Trolox 500uM	Trolox 1mM	Trolox 1mM
Methionine 100uM	Methionine 100uM	Methionine 200uM	Methionine 200uM	Methionine 100uM	Methionine 100uM	Methionine 200uM	Methionine 200uM
Ascorbic Acid 250uM	Ascorbic Acid 250uM			Ascorbic Acid 250uM	Ascorbic Acid 250uM		
Just Cells				Just Cells			
Blank	Media	Control	Control				

250uM H$_2$O$_2$				500uM H$_2$O$_2$			
27	28	29	25	27	29	27	28
31	26	26	26	18	18	20	20
30	27			27	28		
30				16			
1	0	28	28				

Table A2: Statistical analysis of precent calcium per area between all groups day 4.

Group	N	Missing	Median	25%	75%
Ascorbic Acid Day 4	11	0	0.000610	0.000318	0.00126
Trolox Day 4	15	0	0.00651	0.00346	0.00958
Methionine Day 4	12	0	0.0135	0.00886	0.0181
Control Day 4	10	0	0.0248	0.0169	0.0459

Comparison	Diff of Ranks	Q	P	P<0.050
Control Day 4 vs Ascorbic Acid	34.900	5.705	<0.001	Yes
Control Day 4 vs Trolox Day 4	19.833	3.470	0.003	Yes
Control Day 4 vs Methionine Da	8.817	1.471	0.848	No
Methionine Da vs Ascorbic Acid	26.083	4.463	<0.001	Yes
Methionine Da vs Trolox Day 4	11.017	2.032	0.253	No
Trolox Day 4 vs Ascorbic Acid	15.067	2.711	0.040	Yes

Table A3: Statistical analysis of precent calcium per area between all groups day 7.

Group	N	Missing	Median	25%	75%
Ascorbic Acid Day 7	8	0	0.00119	0.000370	0.00286
Trolox Day 7	10	0	0.0247	0.0155	0.0321
Methionine Day 7	14	0	0.0590	0.0444	0.0774
Control Day 7	12	0	0.0820	0.0553	0.0923

Comparison	Diff of Ranks	Q	P	P<0.050
Control Day 7 vs Ascorbic Acid	30.417	5.188	<0.001	Yes
Control Day 7 vs Trolox Day 7	20.917	3.803	<0.001	Yes
Control Day 7 vs Methionine Da	6.702	1.326	1.000	No
Methionine Da vs Ascorbic Acid	23.714	4.165	<0.001	Yes
Methionine Da vs Trolox Day 7	14.214	2.673	0.045	Yes
Trolox Day 7 vs Ascorbic Acid	9.500	1.559	0.714	No

Live/Dead of aggregates with and without AA supplementation:

With AA day 4 (scalebar =100µm):
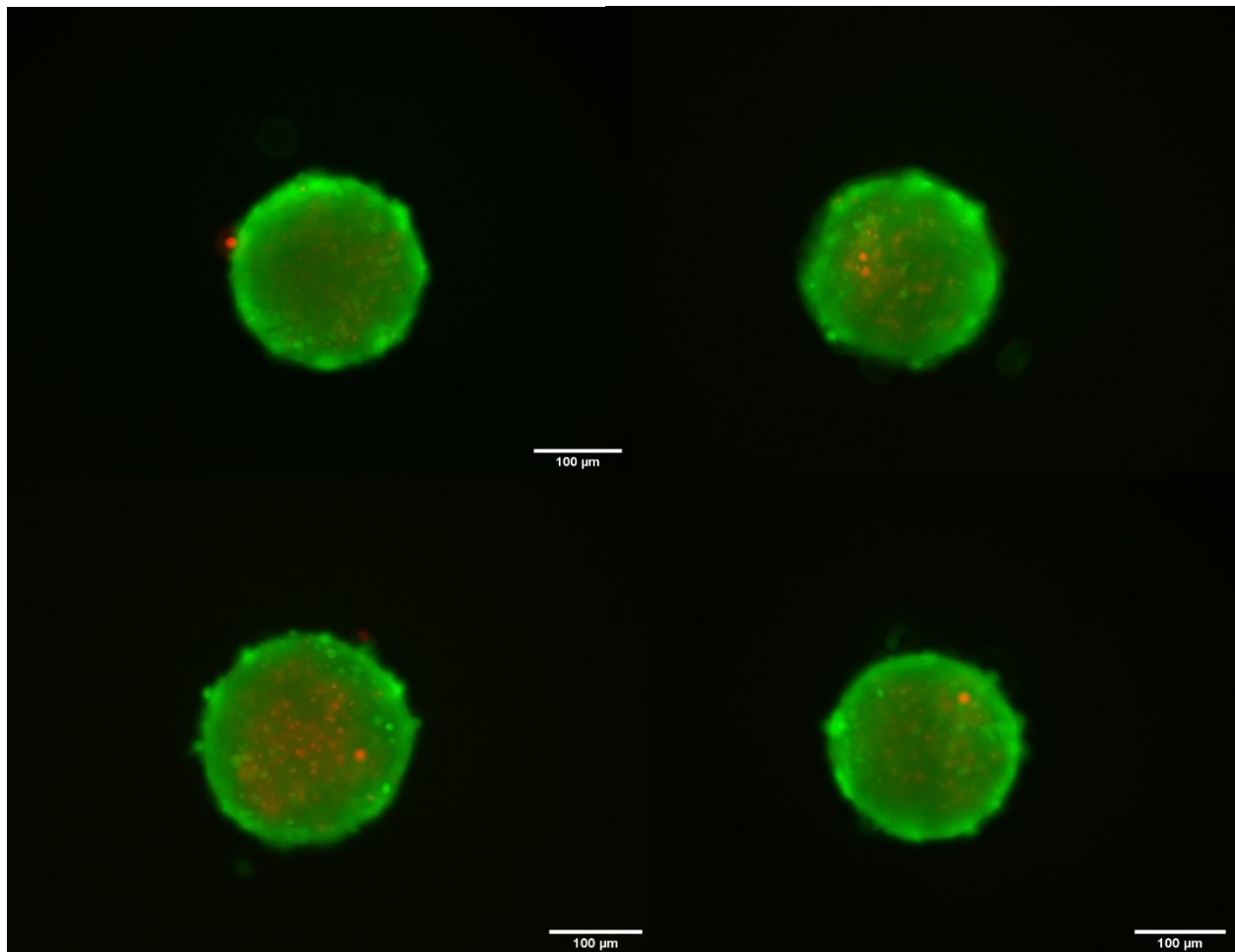
Figure A1: Day 4 porcine aortic VIC aggregates supplemented with 250µM AA revealing minimal dead cells. Any cell death is however primarily in the center of aggregates. Images are supplementary to Figure 8.

Without AA day 4 (scalebar =100µm):
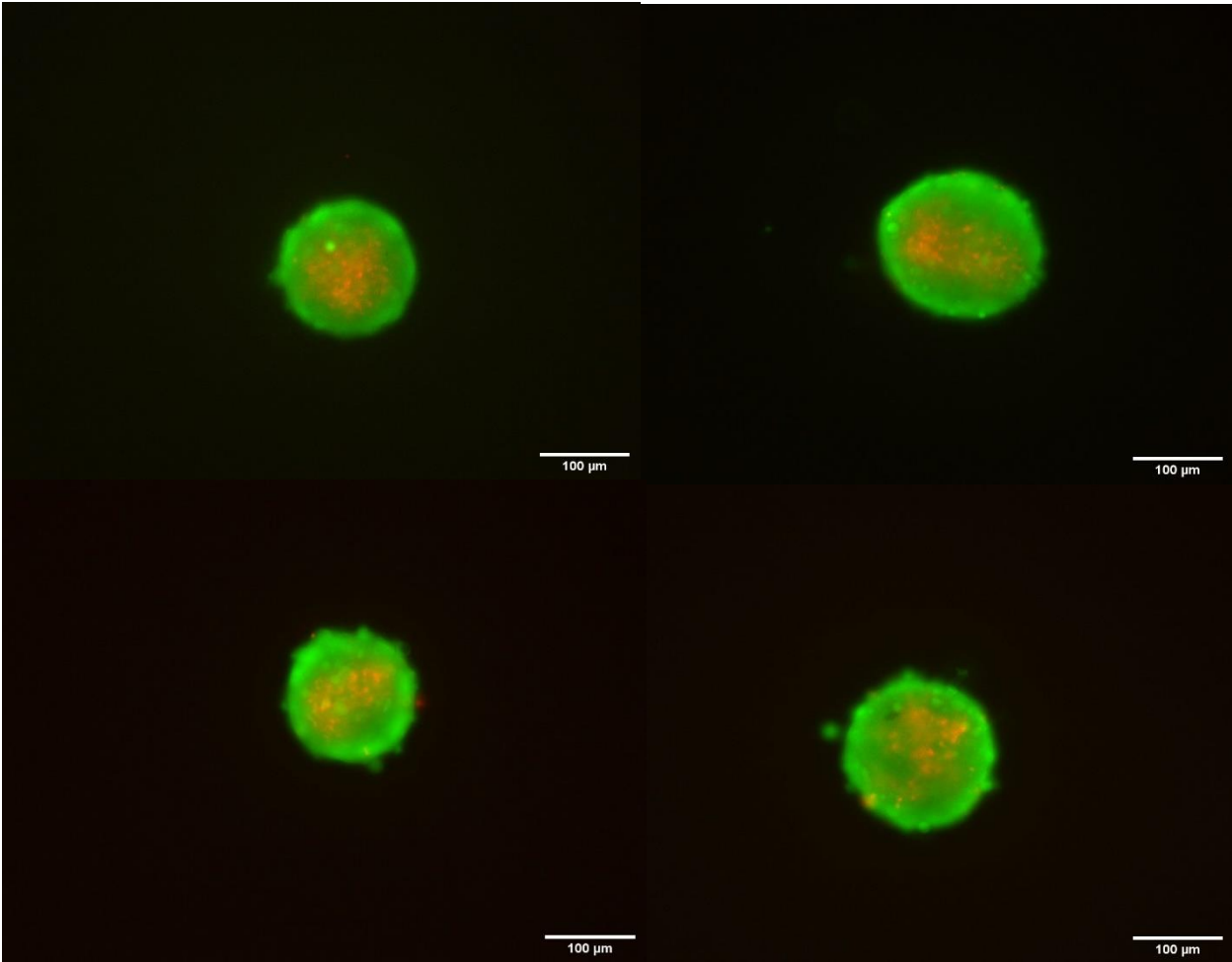
Figure A2: Day 4 porcine aortic VIC aggregates cultured in control media revealing more cell death than aggregates treated with AA. Once again, any cell death is primarily in the center of aggregates. Images are supplementary to Figure 8.

Blocking Apoptosis Through Z-VAD Experiment
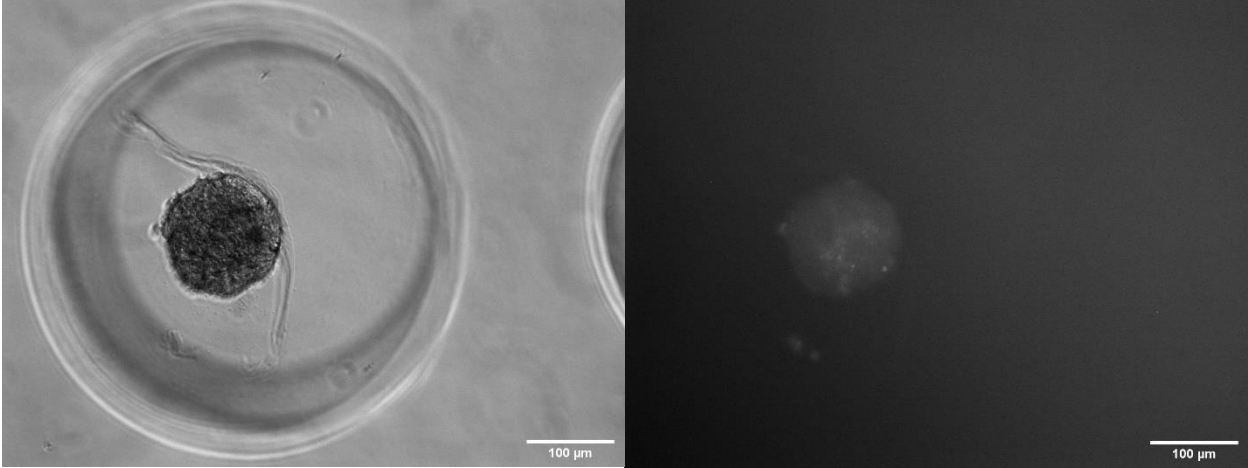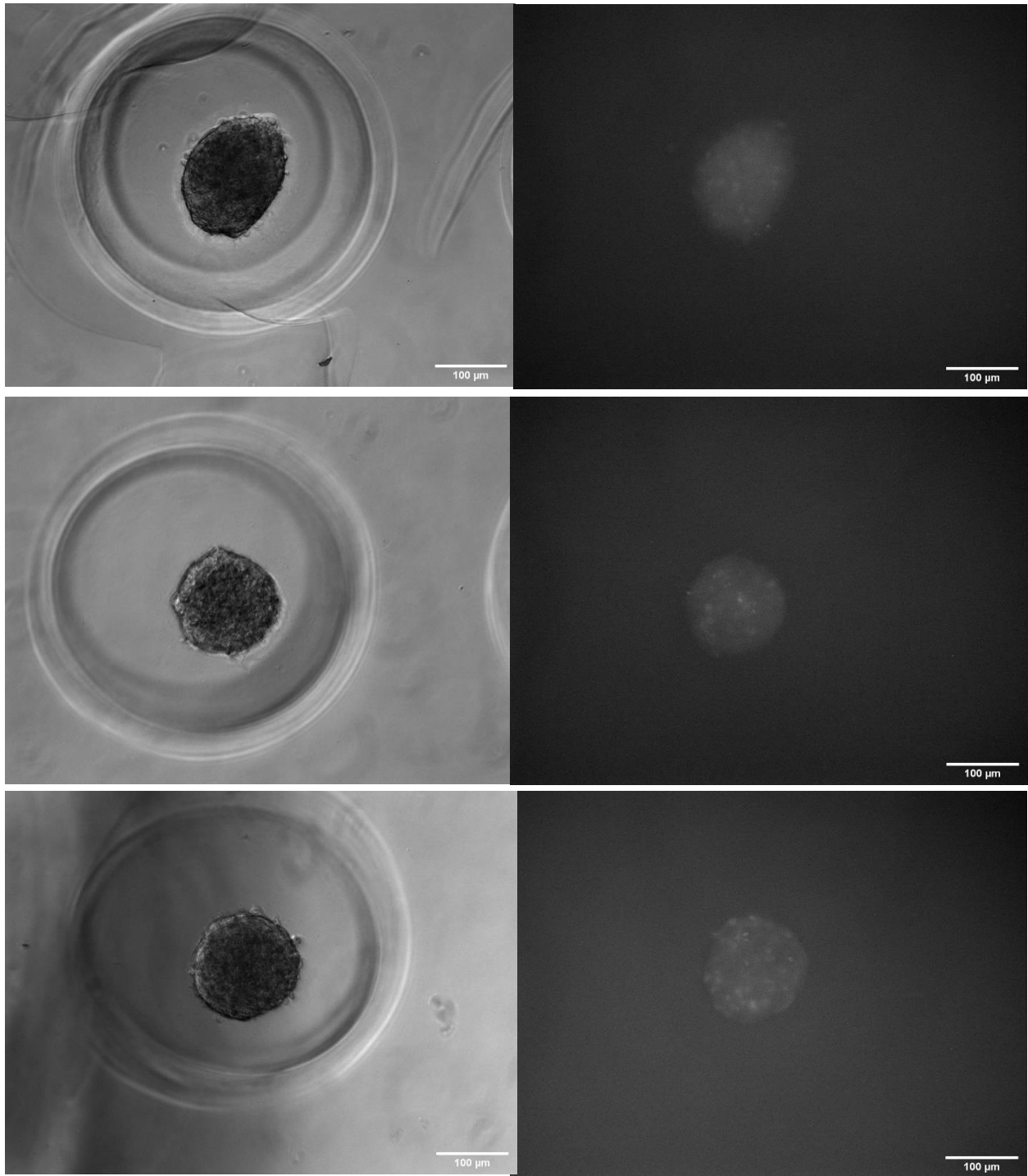
Figure A3: Day 4 porcine aortic VIC aggregates supplemented with Z-VAD. Phase image (left) and Caspase (right) of the same Passage 9 aggregate. The 8 Images are supplementary to Figure 9.
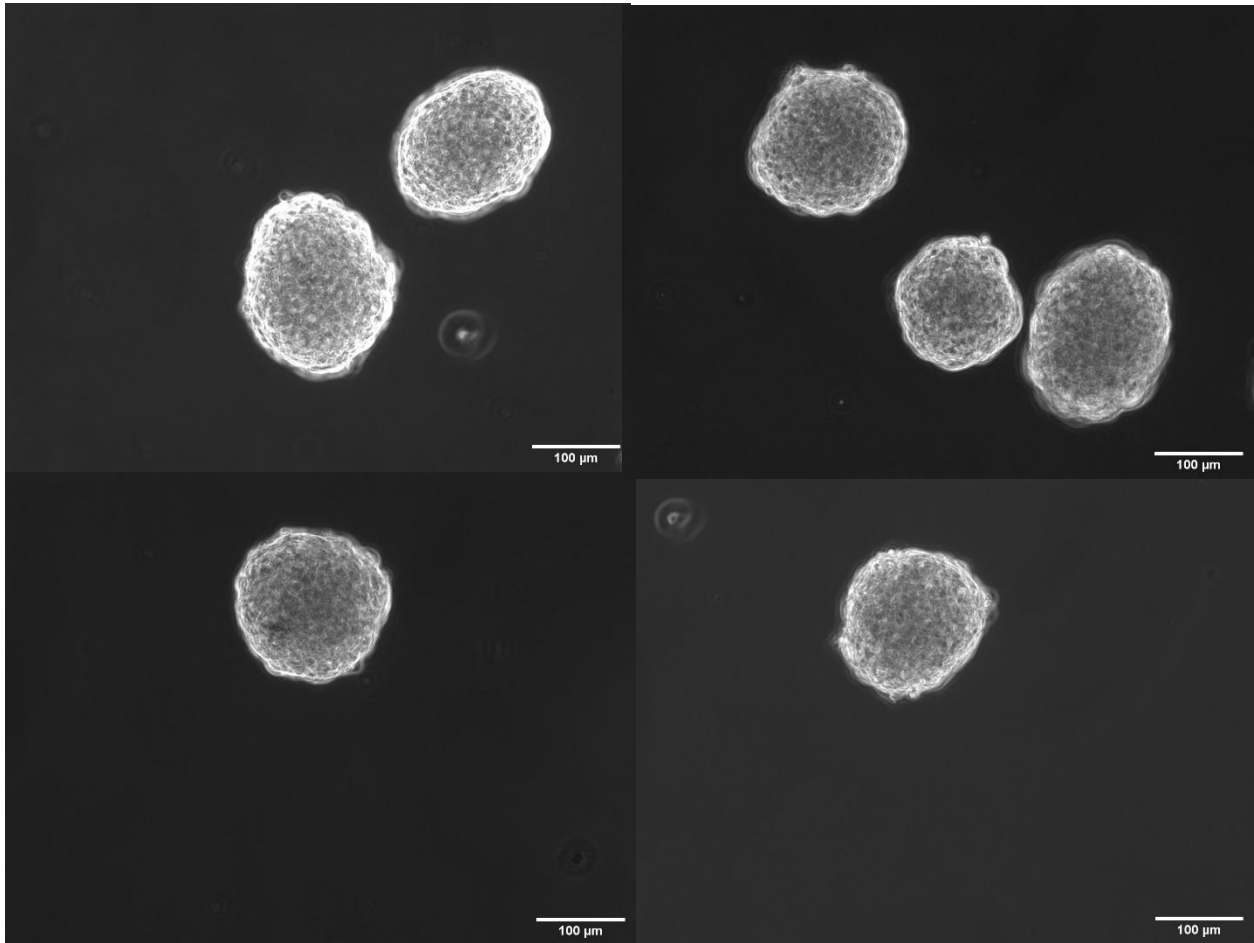
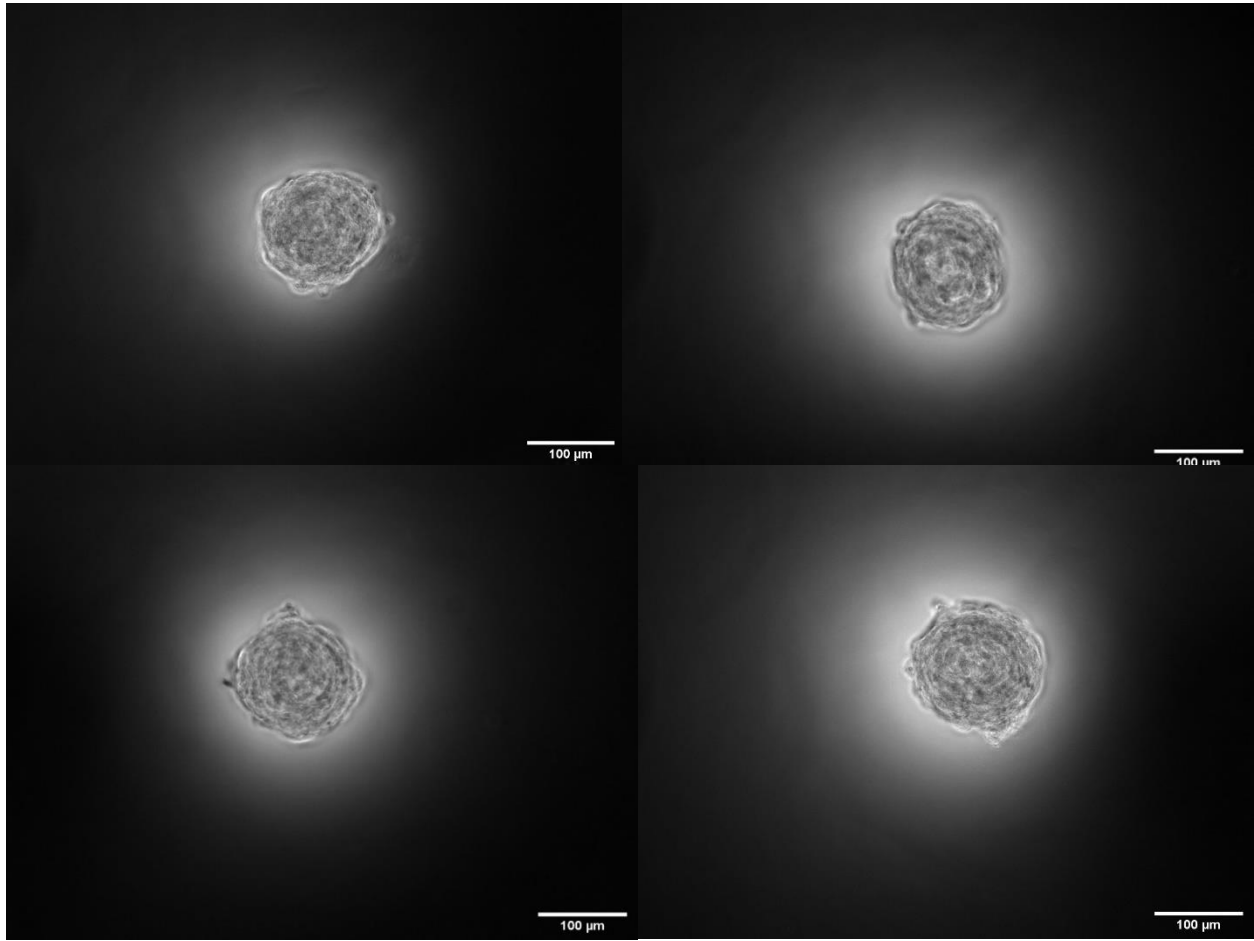*Figure A4: Day 4 passage 9 Von Kossa stain of Z-VAD supplemented porcine aortic VIC aggregates. Images are supplementary to Figure 11.*
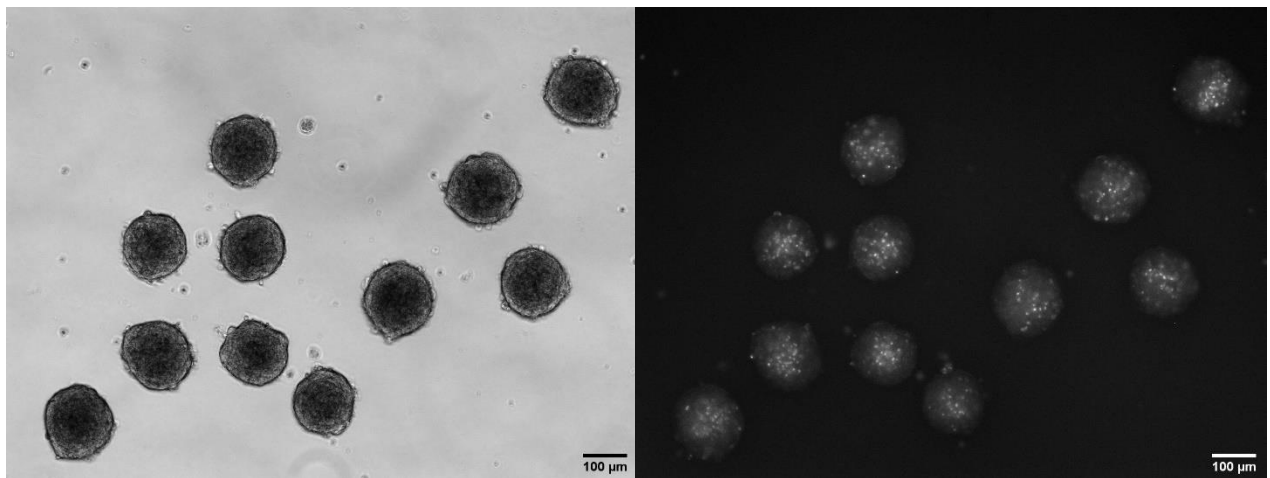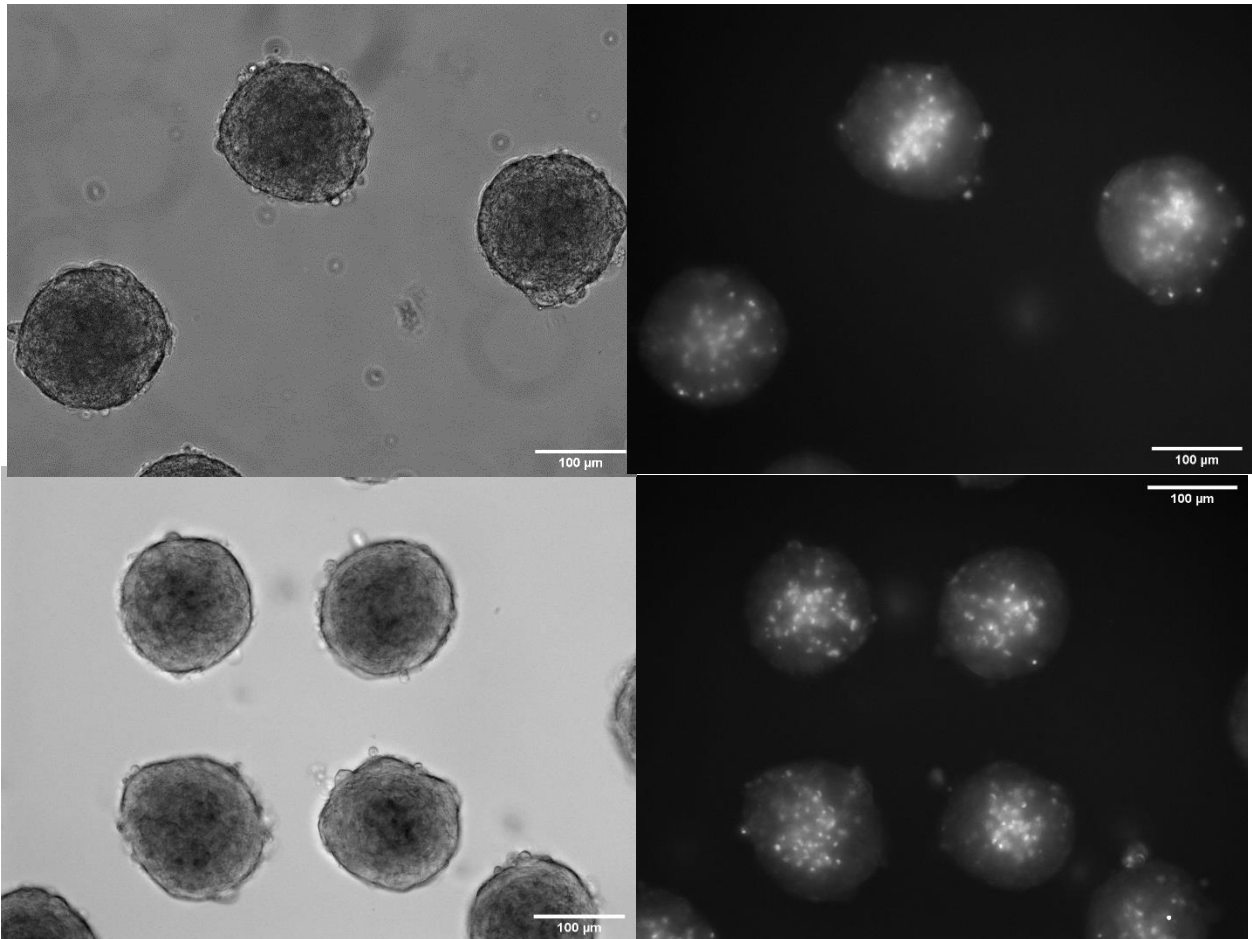
*Figure A5: Day 2 Phase image (left) and Caspase (right) of the same passage 5 porcine aortic VIC aggregate. The 6 Images are supplementary to Figure 10.*
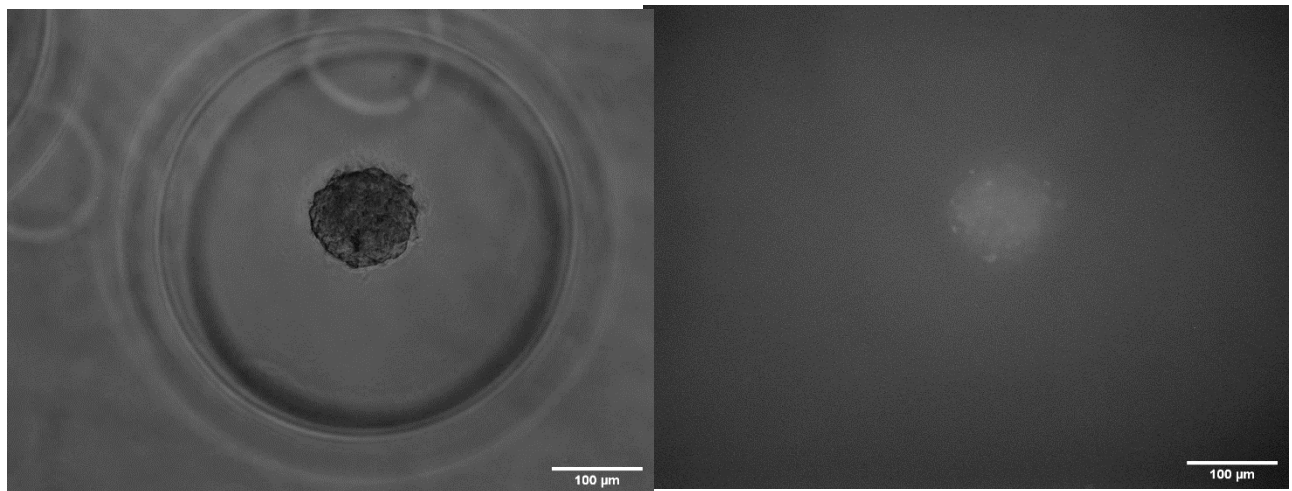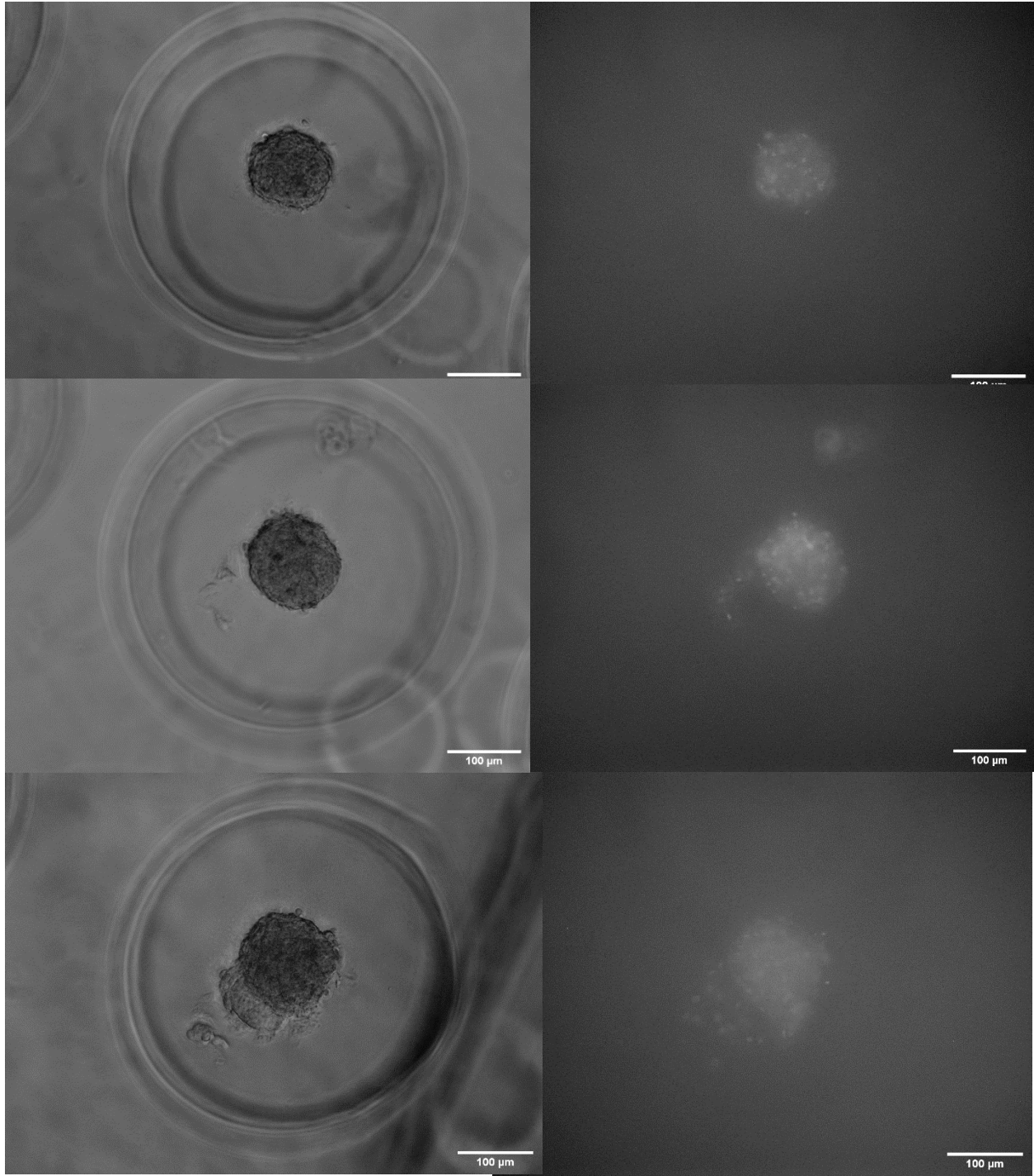
Figure A6: Day 7 Phase image (left) and Caspase (right) of the same passage 9 porcine aortic VIC aggregate. The 8 Images are supplementary to Figure 12.

Figure A7: Day 7 passage 9 Von Kossa stain of Z-VAD supplemented porcine aortic VIC aggregates. Images are supplementary to Figure 13.

Antioxidant Testing Von Kossa Stain:
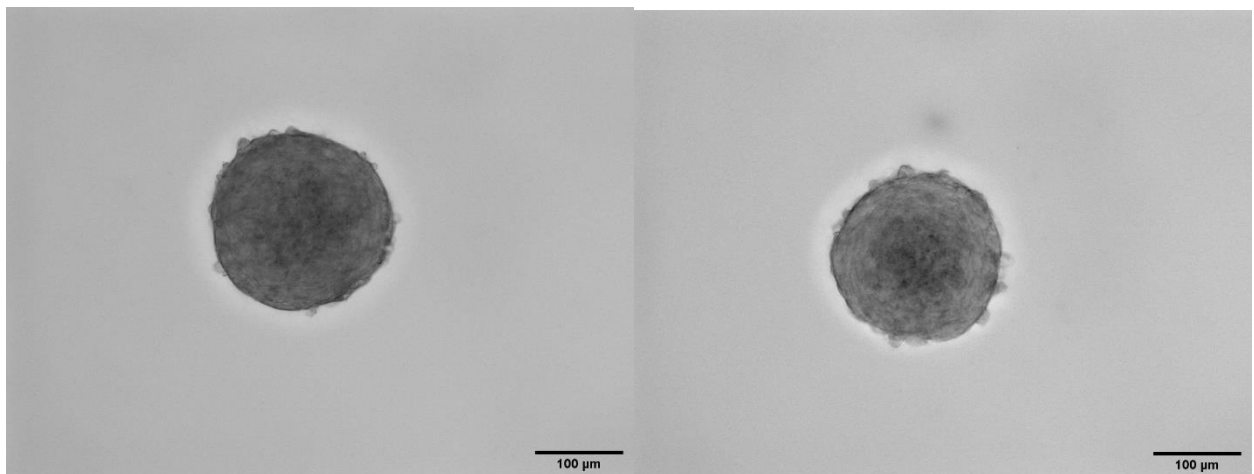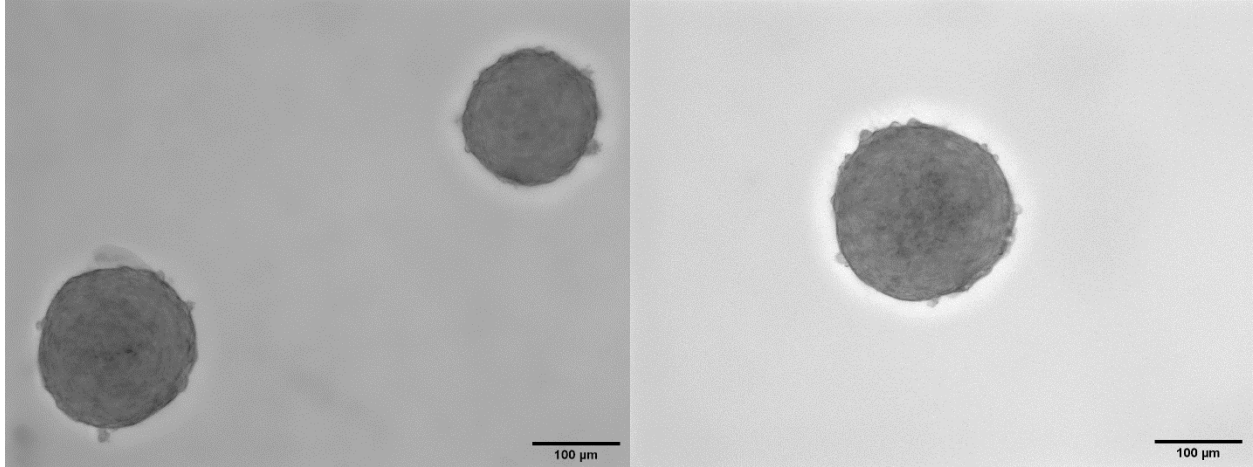
Figure A8: Ascorbic Acid 250µM day 4 passage 4 of porcine aortic VIC aggregates stained with Von Kossa. The 4 Images are supplementary to Figure 16.
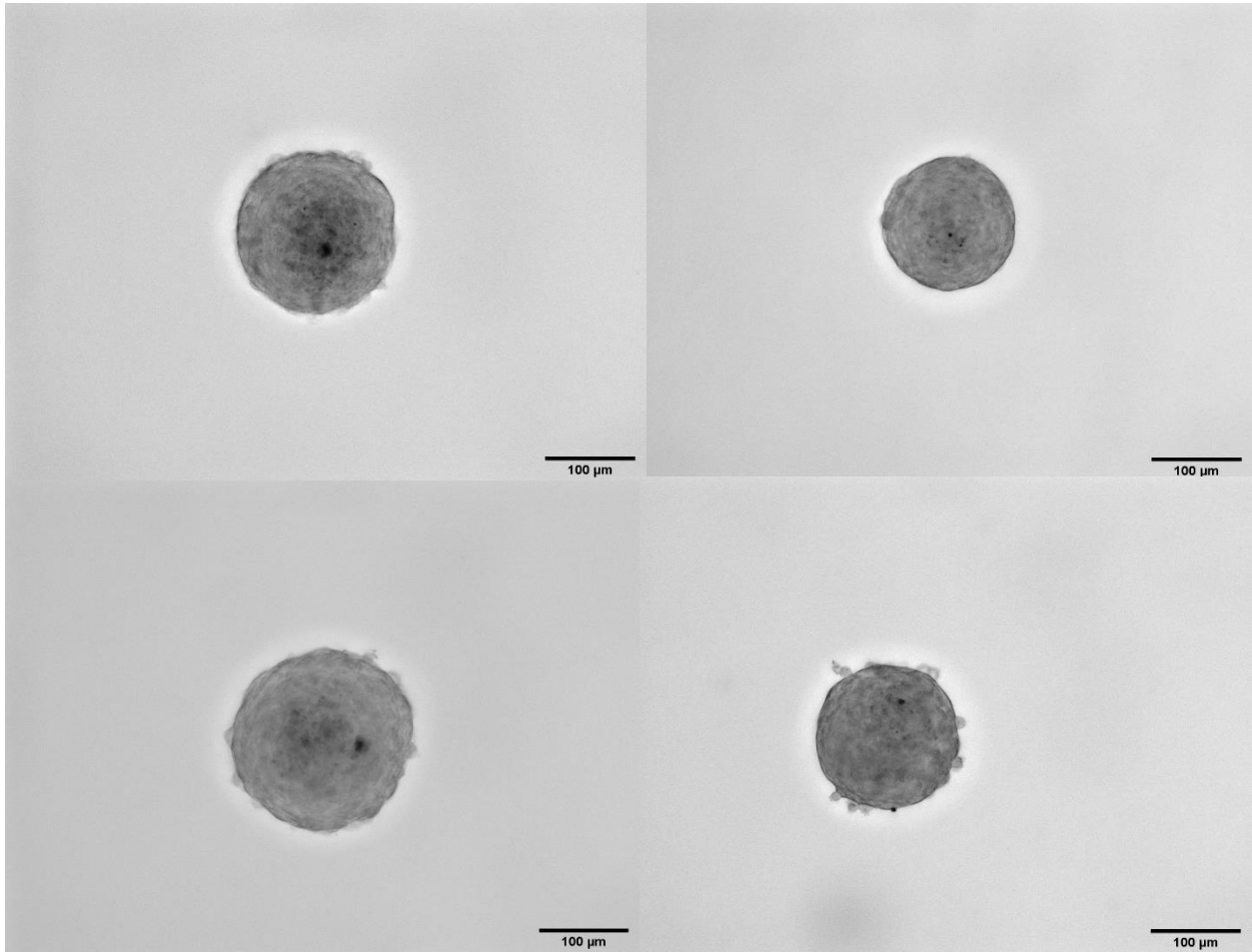

Figure A9: Trolox 500mM day 4 passage 4 of porcine aortic VIC aggregates stained with Von Kossa. Images are supplementary to Figure 16.
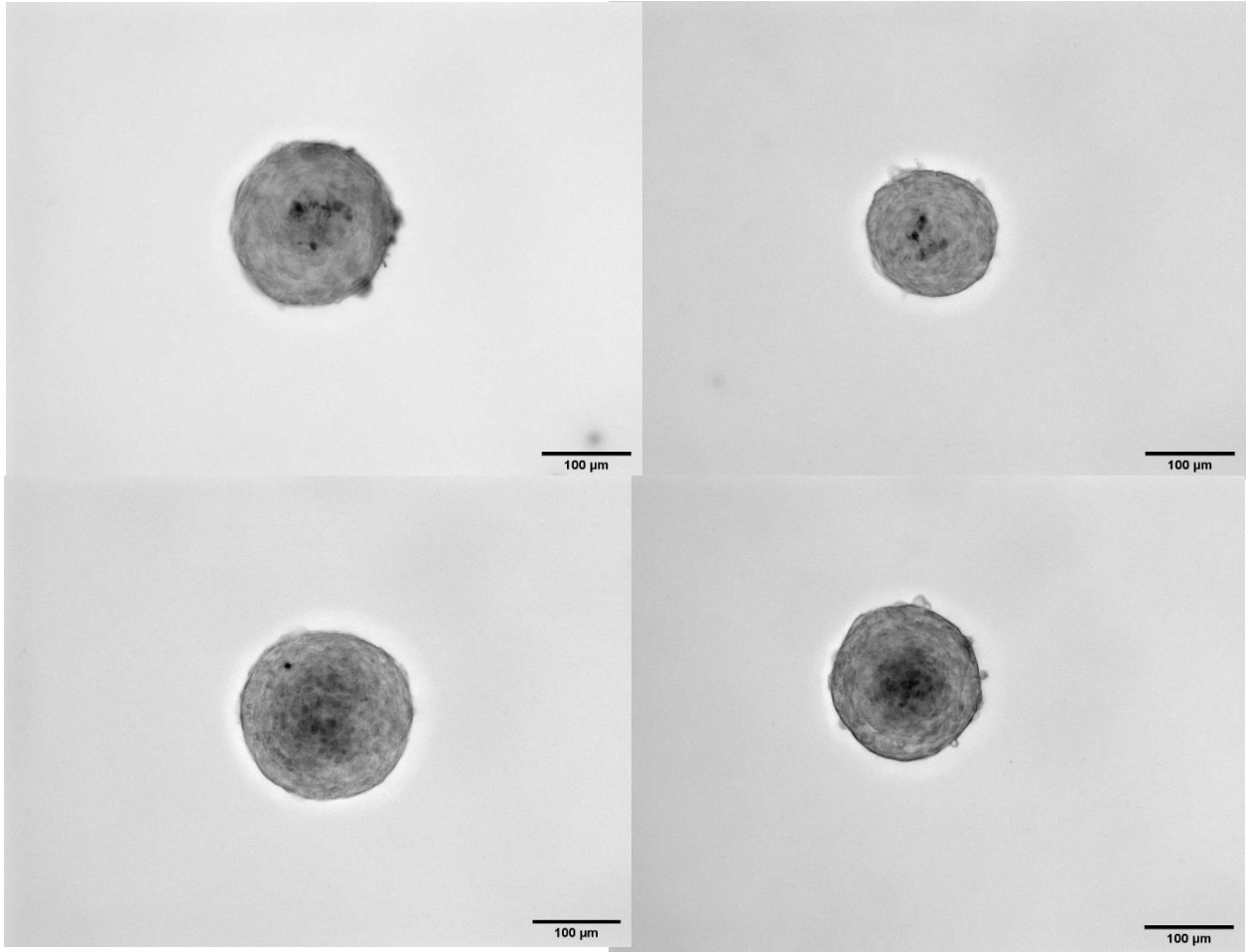
Figure A10: Methionine 200µM day 4 passage 4 of porcine aortic VIC aggregates stained with Von Kossa. Images are supplementary to Figure 16.
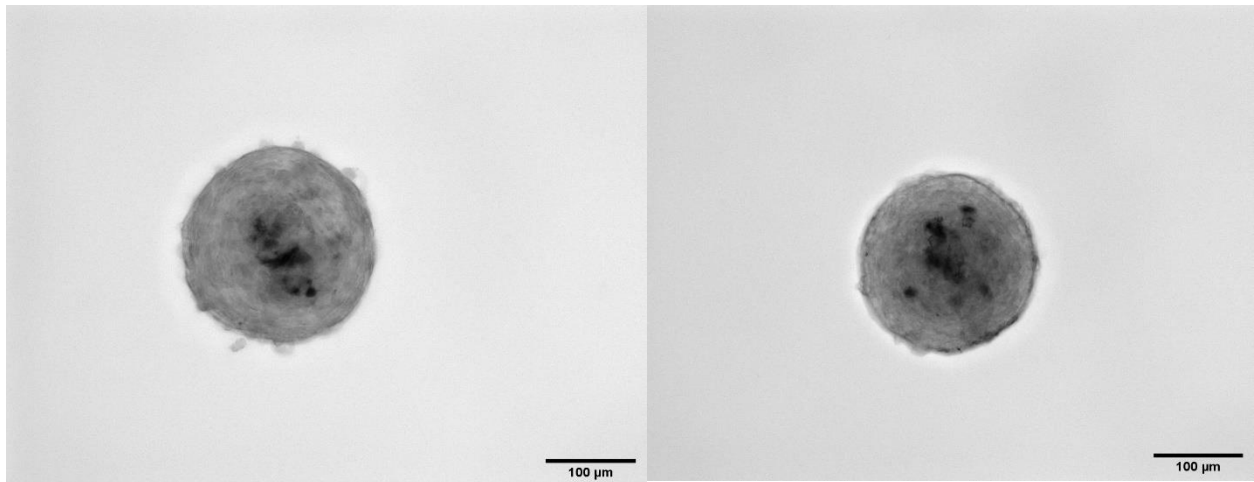
Figure A11: Control day 4 passage 4 of porcine aortic VIC aggregates stained with Von Kossa. The 4 Images are supplementary to Figure 16.
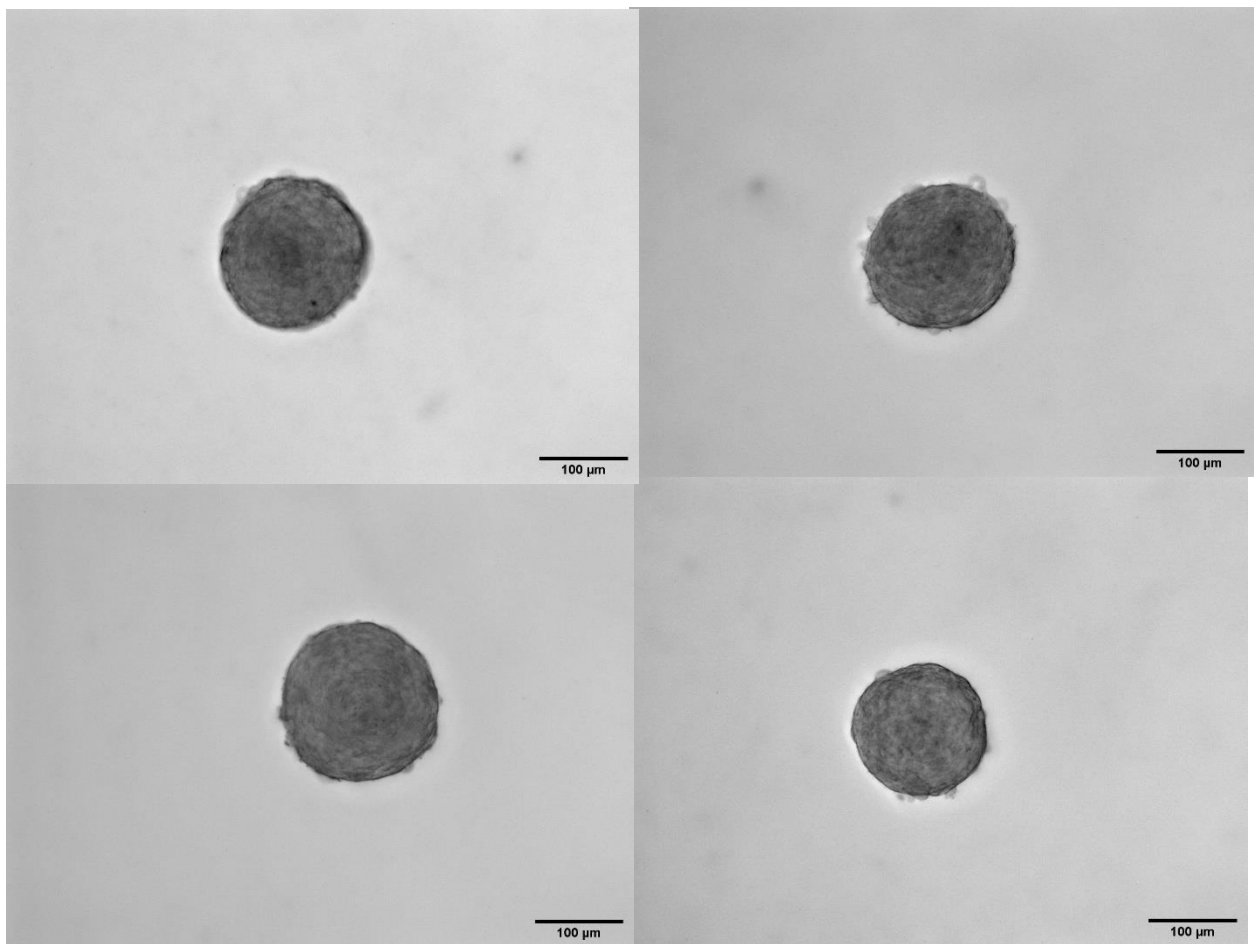

Figure A12: Ascorbic Acid 250µM day 7 passage 4 of porcine aortic VIC aggregates stained with Von Kossa. Images are supplementary to Figure 17.
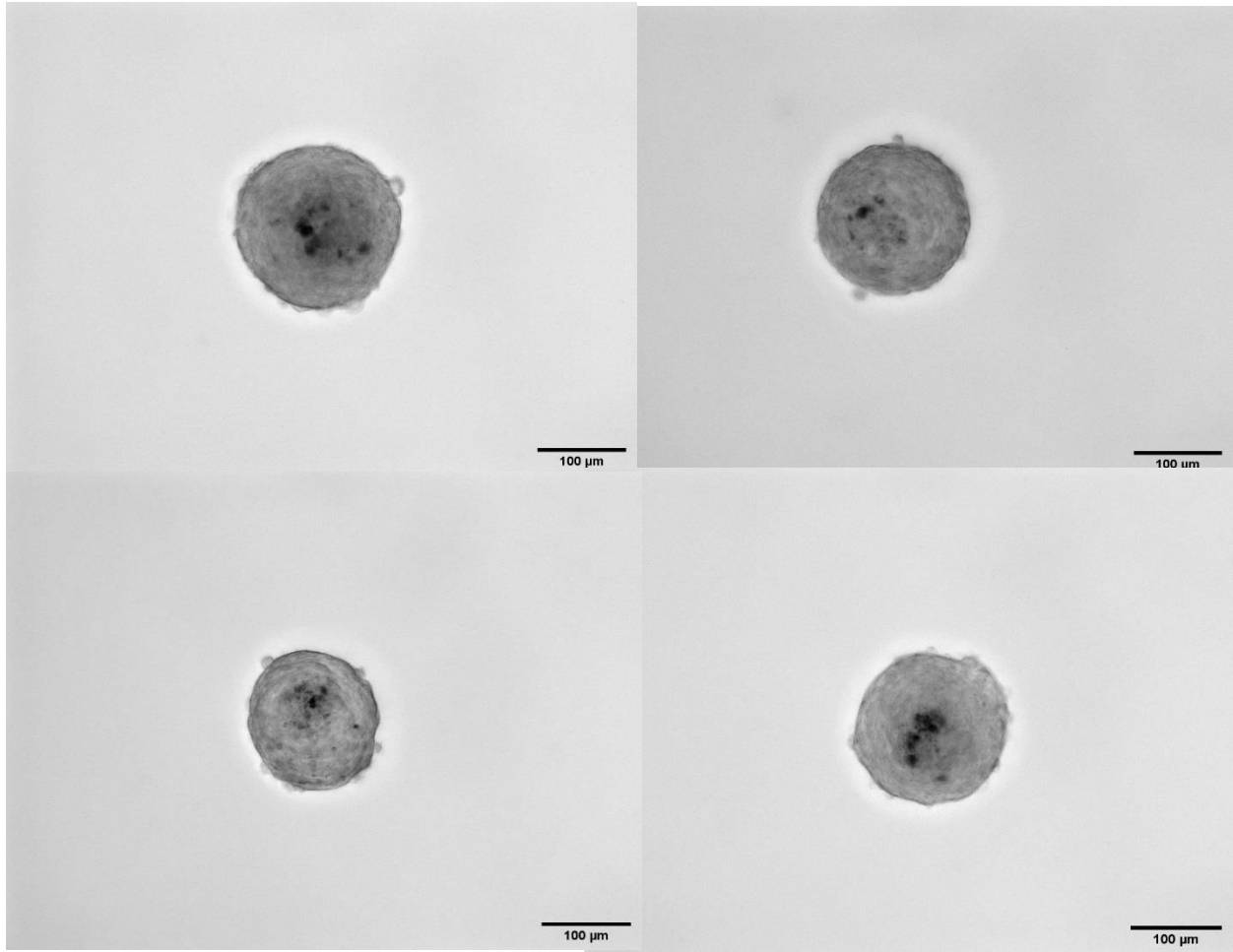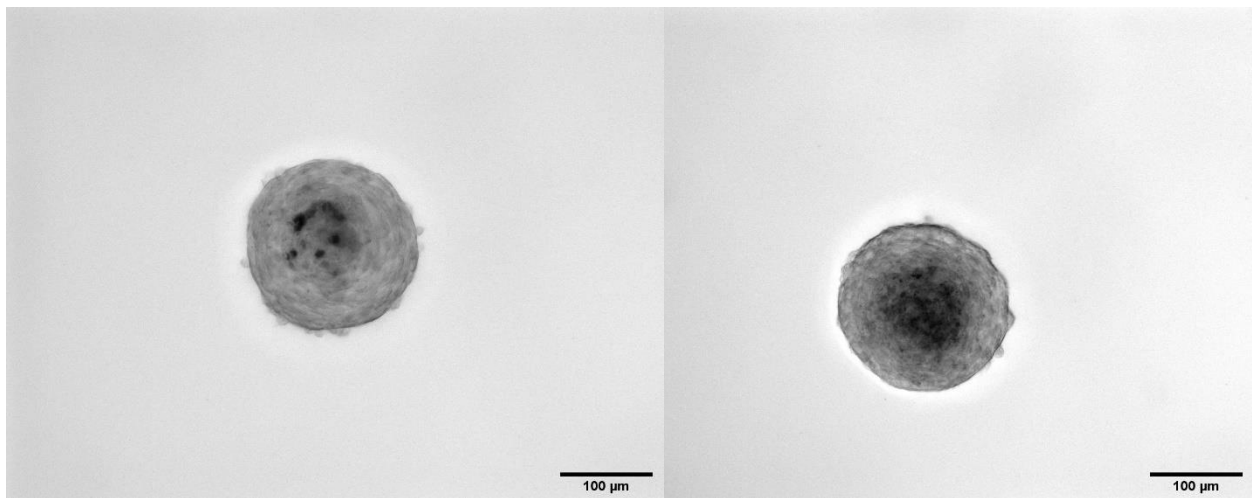
Figure A13: Trolox 500mM day 7 passage 4 of porcine aortic VIC aggregates stained with Von Kossa. Images are supplementary to Figure 17.
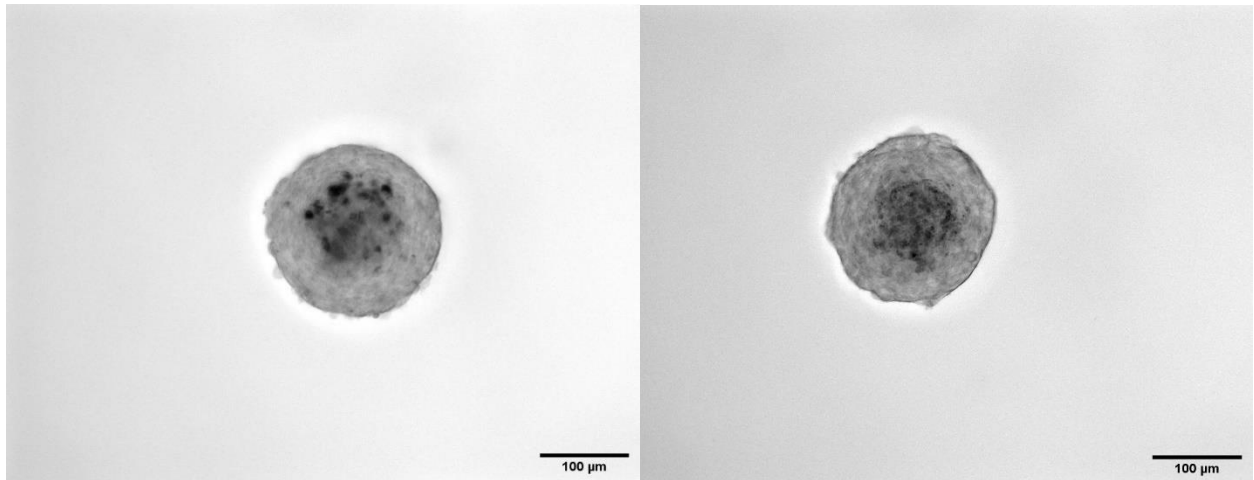
Figure A14: Methionine 200μM day 7 passage 4 of porcine aortic VIC aggregates stained with Von Kossa. The 4 Images are supplementary to Figure 17.
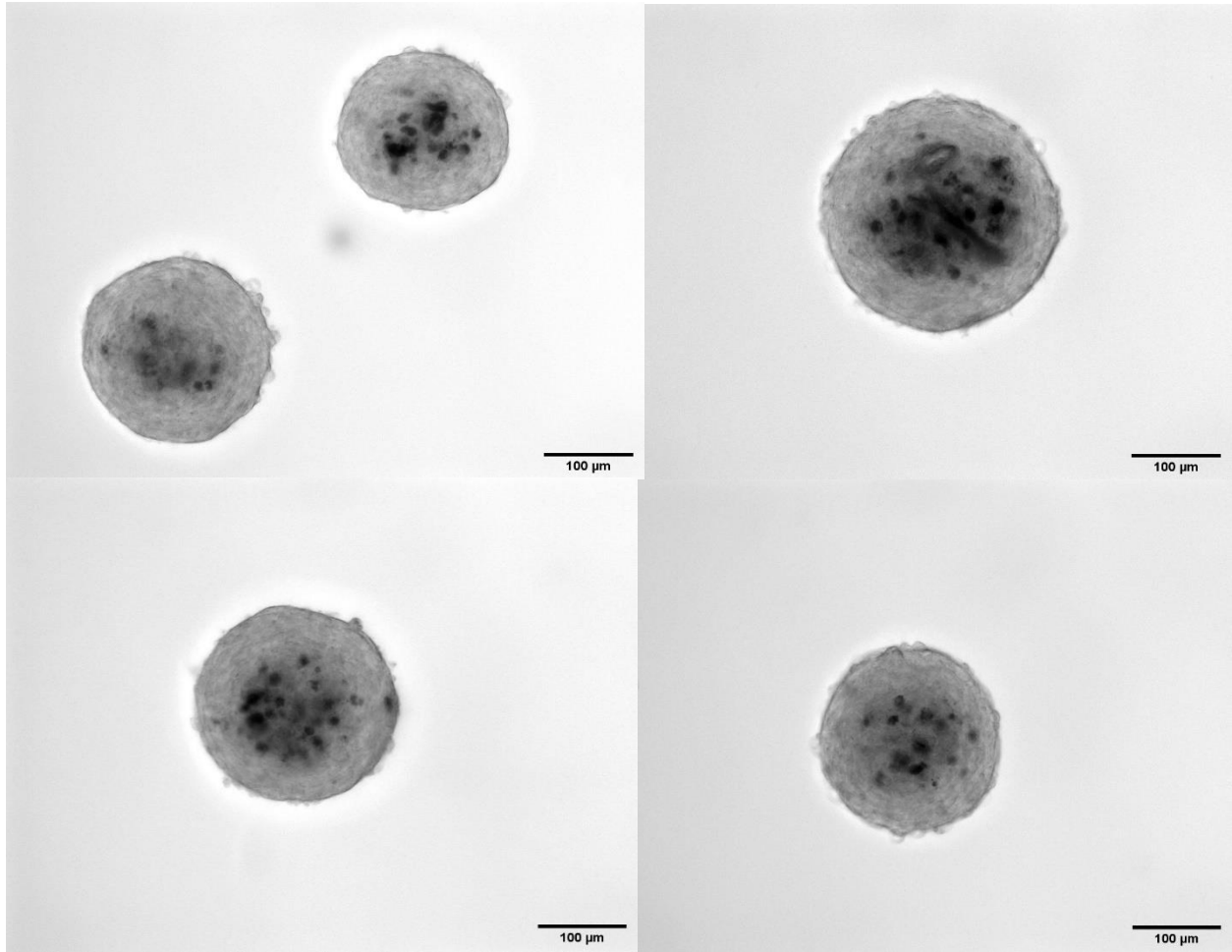

Figure A15: Control day 7 passage 4 of porcine aortic VIC aggregates stained with Von Kossa. Images are supplementary to Figure 17.

Table A4: The data of aggregate size with the antioxidant supplement revealing no significant difference in sizes of the aggregates on the same day and a slight decrease in size from day 4 to day 7.

Day 4 AA	Day 4 Trolox	Day 4 Methionine	Day 4 Control
110,500$\pm$24,300 μm^2	103,300$\pm$15,000 μm^2	102,100$\pm$15,300 μm^2	110,000$\pm$26,000 μm^2
Day 7 AA	Day 7 Trolox	Day 7 Methionine	Day 7 Control
99,700$\pm$21,200 μm^2	96,700$\pm$18,000 μm^2	97,600$\pm$11,500 μm^2	98,800$\pm$18,900 μm^2

Table A5: Further descriptions of various models currently used to study CAVD. Unless otherwise specified, models are single cell and not aggregated cells.
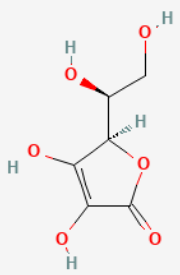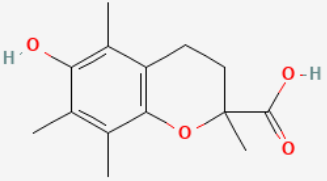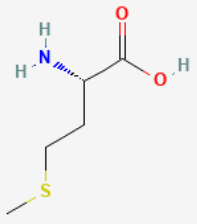
Research Group	2D or 3D	Polymer/System	Cell Type/Media	Major Findings
Merryman group Fisher, C.I., J. Chen, and W.D. Merryman, *Calcific nodule morphogenesis by heart valve interstitial cells is strain dependent.* Biomech Model Mechanobiol, 2013. **12**(1): p. 5-17.	2D	Bioflex Pronectin culture plates	Porcine aortic VIC/ TGF-β1	Apoptosis proceeded calcific nodule formation. Continual exposure to strain accelerates aggregates to calcify into mature nodules.
Leinwand group Walker, G.A., et al., *Valvular myofibroblast activation by transforming growth factor-beta: implications for pathological extracellular matrix remodeling in heart valve disease.* Circ Res, 2004. **95**(3): p. 253-60.	2D	free-floating and stressed (mechanically loaded) collagen matrices	Porcine aortic VIC/ TGF-β1	Transforming growth factor-β1 (TGF-β1) mediates differentiation of VICs into active myofibroblasts in vitro in a dose-dependent manner.
Simmons group Yip, C.Y., et al., *Calcification by valve interstitial cells is regulated by the stiffness of the extracellular matrix.* Arterioscler Thromb Vasc Biol, 2009. **29**(6): p. 936-42.	2D	Constrained collagen gel	Porcine aortic VIC/ osteogenic and TGF-β1	Apoptosis precedes calcification. Also, stiffer substrates promote calcification.

Billiar group Cirka, H.A., et al., *Reproducible in vitro model for dystrophic calcification of cardiac valvular interstitial cells: insights into the mechanisms of calcific aortic valvular disease.* Lab Chip, 2017. **17**(5): p. 814-829.	2D	Microcontact printing with collagen to form aggregates	Porcine aortic VIC/ normal	Capable of forming highly reproducible aggregates where 70% stained positive for Alizarin Red after one week in culture, and mineralized calcium-positive nanoparticles were found within the VIC aggregates.
Aikawa group Goto, S., Rogers, M. A., Blaser, M. C., Higashi, H., Lee, L. H., Schlotter, F., Body, S. C., Aikawa, M., Singh, S. A., & Aikawa, E. (2019). Standardization of Human Calcific Aortic Valve Disease *in vitro* Modeling Reveals Passage-Dependent Calcification. *Frontiers in cardiovascular medicine*, 6, 49.	2D	48-well culture plate	Human aortic VIC/ osteogenic and pro-calcifying	Media culture conditions and VIC passage numbers impact the calcification potential
Merryman group Hutcheson, J. D., et al. (2012). *Cadherin-11 regulates cell-cell tension necessary for calcific nodule formation by valvular myofibroblasts.* Arteriosclerosis, Thrombosis, and Vascular Biology.	2D	Tissue culture dishes with induced cell aggregation	Porcine aortic VIC/ TGF-β1	There is a necessity of cadherin-11 for dystrophic calcific nodule formation, which proceeds through an Erk1/2-dependent pathway.
Merryman group Chen, J., Peacock, J. R., Branch, J., & David Merryman, W. (2015). Biophysical analysis of	2D	Tissue culture dishes with induced cell aggregation	Porcine aortic VIC/ osteogenic and TGF-β1	There are distinct differences between the nodule types of dystrophic and osteogenic calcification.

dystrophic and osteogenic models of valvular calcification. *Journal of biomechanical engineering*, *137*(2), 020903.				
Butcher group

Duan, B., et al., *Active tissue stiffness modulation controls valve interstitial cell phenotype and osteogenic potential in 3D culture.* Acta Biomater, 2016. **36**: p. 42-54. | 3D | HA hydrogel with adjustable stiffness | Human aortic VIC/ osteogenic and TGF-β1 | That constructs with initially valve leaflet layer-like stiffness significantly promote myofibroblastic phenotype. |
| Aikawa group

Hjorntaes, J., et al., *Simulation of Early Calcific Aortic Valve Disease in a 3D Platform: A Role For Myofibroblast Differentiation.* 2016: Journal or Molecular and Cellular Cardiology. p. 13-20. | 3D | Photo-crosslinked hyaluronic acid and gelatin | Porcine aortic VIC/ osteogenic | Myofibroblast-like response only occurs when exposed to exogenous environmental cues, and there was no apoptotic driven calcification. |
| Grande-Allen group

Monroe, M.N., R.C. Nikonowicz, and K.J. Grande-Allen, *Heterogeneous multi-laminar tissue constructs as a platform to evaluate aortic valve matrix-dependent pathogenicity.* Acta Biomater, 2019. **97**: p. 420-427. | 3D | laminar, filter paper-based cell culture system | Porcine aortic VIC/ normal | The relative amount of fibrillar collagen within a 3D construct dictates the osteogenic capacity of VICs that reside in the construct. |
| Nerem group

Butcher, J.T. and R.M. Nerem, *Porcine aortic valve interstitial cells in three-dimensional culture: comparison of phenotype with aortic smooth muscle cells.* J Heart Valve Dis, | 3D | collagen I solution which formed a fibrillar gel network | Porcine aortic VIC/ normal | Differences in protein and GAG content indicated an ability of the valvular interstitial cell to synthesize matrix in 3D culture, without the need of biochemical or |

2004. **13**(3): p. 478-85; discussion 485-6.				mechanical stimulation.
Anseth group Mabry, K.M., R.L. Lawrence, and K.S. Anseth, Dynamic stiffening of poly(ethylene glycol)-based hydrogels to direct valvular interstitial cell phenotype in a three-dimensional environment. Biomaterials, 2015. 49: p. 47-56.	3D	MMP-degradable, PEG-based hydrogels using a photoinitiated thiol-ene reaction	Porcine aortic VIC/ TGF-β1	Substrate modulus had an influence on VIC morphology and calcification, where stiffer substrates lead higher levels of calcium deposition.
Vaage group Zabirnyk, A., et al., *A Novel Ex Vivo Model of Aortic Valve Calcification. A Preliminary Report.* Front Pharmacol, 2020. 11: p. 568764.	3D	Dissected porcine aorta cultured in osteogenic media	Whole valve/osteogenic media	They were only able to induce calcification with osteogenic supplementation.
Butcher group Terence W. Gee, Jennifer M. Richards, Ablajan Mahmut, Jonathan T. Butcher, Valve endothelial-interstitial interactions drive emergent complex calcific lesion formation in vitro, Biomaterials, Volume 269, 2021, 120669, ISSN 0142-9612	3D	Cellularized type I collagen hydrogels in PDMS circular wells for inducing mechanical stress	Porcine aortic VIC and valvular endothelial cells (VEC)/ osteogenic	Valve endothelial cell coculture exacerbates valve interstitial cell calcific deposition under osteogenic conditions. Valve endothelial cells contribute to valve interstitial cell pathological remodeling and calcification, which denotes an active role of the endothelium in progressive valvular degeneration.

Table A6: Further information regarding the antioxidants used in experiments. The table provides the compound name, chemical structure, molecular weight, Log P, Formal Charge, and Solubility for each antioxidant. All information gained from PubChem [43,44,45].

Antioxidant	Compound Name	Chemical Structure	Molecular Weight	Log P	Formal Charge	Solubility
AA [44]	(5R)-[(1S)-1,2-Dihydroxyethyl]-3,4-dihydroxyfuran-2(5H)-one		176.12 g/mol	-1.85	0	Water Soluble
Trolox [43]	6-hydroxy-2,5,7,8-tetramethylchroman-2-carboxylic acid		250.29 g/mol	−0.805	0	Soluble in DMSO (up to 25 mg/ml) or in Ethanol (up to 25 mg/ml)
Methionine [45]	2-amino-4-(methylthio)butanoic acid		149.21 g/mol	-1.87	0	Water Soluble